GEOLOGICA CARPATHICA, 2026, 77, 5, 371–389 https://doi.org/10.31577/GeolCarp.2026.19

Proterozoic deformation stages of the Earth's crust in the western part of the Ukrainian Shield and their manifestation in magmatism and the distribution of crustal physical properties

SERGII MYCHAK[1,✉], IRINA MAKARENKO[1], OLGA USENKO[1], OLGA LEGOSTAEVA[1], MIROSLAV BIELIK[2,3], JANA DÉREROVÁ[3] and OLEKSII BABYNIN[1]

[1]S. Subbotin Institute of Geophysics of National Academy of Sciences of Ukraine, 32 Akademika Palladina avenue, Kyiv, 03680, Ukraine
[2]Department of Engineering Geology, Hydrogeology and Applied Geophysics, Faculty of Natural Sciences, Comenius University, Mlynská dolina, Ilkovičova 6, 842 15 Bratislava, Slovak Republic
[3]Division of Geophysics, Earth Science Institute of the Slovak Academy of Sciences, Dúbravská cesta 9, 841 04 Bratislava, Slovak Republic

(Manuscript received March 2, 2026; accepted in revised form August 4, 2026; Associate Editor: Ján Vozár)

Abstract: The chronological and spatial relationships between tectonic faulting and magmatic activity of the Earth's crust within the western part of the Ukrainian Shield during the Paleoproterozoic (2.08–1.73 Ga) was investigated. Based on tectonophysical analysis of major fault zones (e.g., Sushchany–Perha, Nemyriv, Khmilnyk, Zvizdal–Zalissia, Brusyliv) and on structural analysis of the Novohrad-Volynskyi granitoid massif and the Korosten Pluton of gabbro–anorthosite and rapakivi granite was delineated discrete stages of tectono-magmatic activity. These stages were accompanied by changes in the regional stress–strain regime and the formation of distinct magmatic complexes. Results of 3D gravity modelling reveal two dominant fault systems – northeast-trending and sub-latitudinal – that control the distribution of structural heterogeneities in the crust. The meridional Bilokorovychi fault zone is established as a structural boundary dividing the western Ukrainian Shield into two parts: western and eastern. Both differ significantly in different density and magnetic properties, as well as in the thickness of the crust. The western part is characterized by thicker crust (up to 60 km), positive regional magnetic anomalies achieving values up to +350 nT and higher densities on Moho (up to 3.12 g cm^{-3}). On the other hand, the eastern part is represented by thinner crust (only 40–50 km), mostly negative magnetic anomalies, which in the space of Korosten Pluton reach values of −350 nT and lower values of the densities on the Moho (2.98–3.06 g cm^{-3}). The data highlight the central role of tectonic faults in building the present crustal structure, reflected in the patterns of the regional magnetic field and in crustal density heterogeneity.

Keywords: Ukrainian Shield, Korosten Pluton, fault zones, magmatism, dykes, 3D density modelling

Introduction

The modern structure of the western part of the Ukrainian Shield (Ush, Fig. 1) formed during the Paleoproterozoic collision of three microcontinents – Fennoscandia, Sarmatia, and Volgo-Uralia – between ca. 2.05–1.73 Ga (Bogdanova et al. 2006, 2013; Shumlyanskyy et al. 2016; Mychak et al. 2023). This interval was marked by sustained strike-slip faulting, deformation, and large-scale magmatism over several tectonic phases. Tectonophysical investigations cover the Podolian, Ros', and Volyn domains. The consolidation and spatial boundary delineation of these domains occurred along a system of inter-domain fault zones that dissect the crystalline basement, which exhibits a heterogeneous structure (Gintov et al. 2018).

The southern part of the study area is represented by the Archean Podolian Domain (Bogdanova et al. 2013). It is a stable terrane composed of rocks of the Dniester–Buh and Buh series, metamorphosed under granulite facies conditions (Shcherbakov 2005).

The eastern flank encompasses the Ros' Domain, whose Archean basement underwent profound Paleoproterozoic tectonomagmatic reworking, resulting in the development of the Ros'–Tikych series (Shcherbakov 2005). A common feature of both domains is the widespread occurrence of granites aged 2.2–2.0 Ga (Shcherbak et al. 2008).

To the northwest lies the Volyn Domain, which developed as a Paleoproterozoic orogen composed of volcano-sedimentary and granitoid complexes. Within the framework of these geodynamic events, the Teteriv–Zhytomyr orogenic belt (2.15–2.05 Ga) and the Osnytsk–Mikashevychi igneous belt (OMIB; 2.00–1.95 Ga) developed in the boundaries of the Volyn Domain (Shumlyanskyy 2014; Shumlyanskyy et al. 2017; Stepanyuk et al. 2020; Usenko 2024, 2025). The former comprises metapelitic sedimentary, carbonate, and diverse metavolcanic rocks metamorphosed to amphibolite facies, autochthonous granites, and numerous granite intrusions. From a tectonophysical perspective, the entire sequence of these structural and magmatic events marks a prolonged

✉ corresponding author: Sergii Mychak
sergiimychak@gmail.com

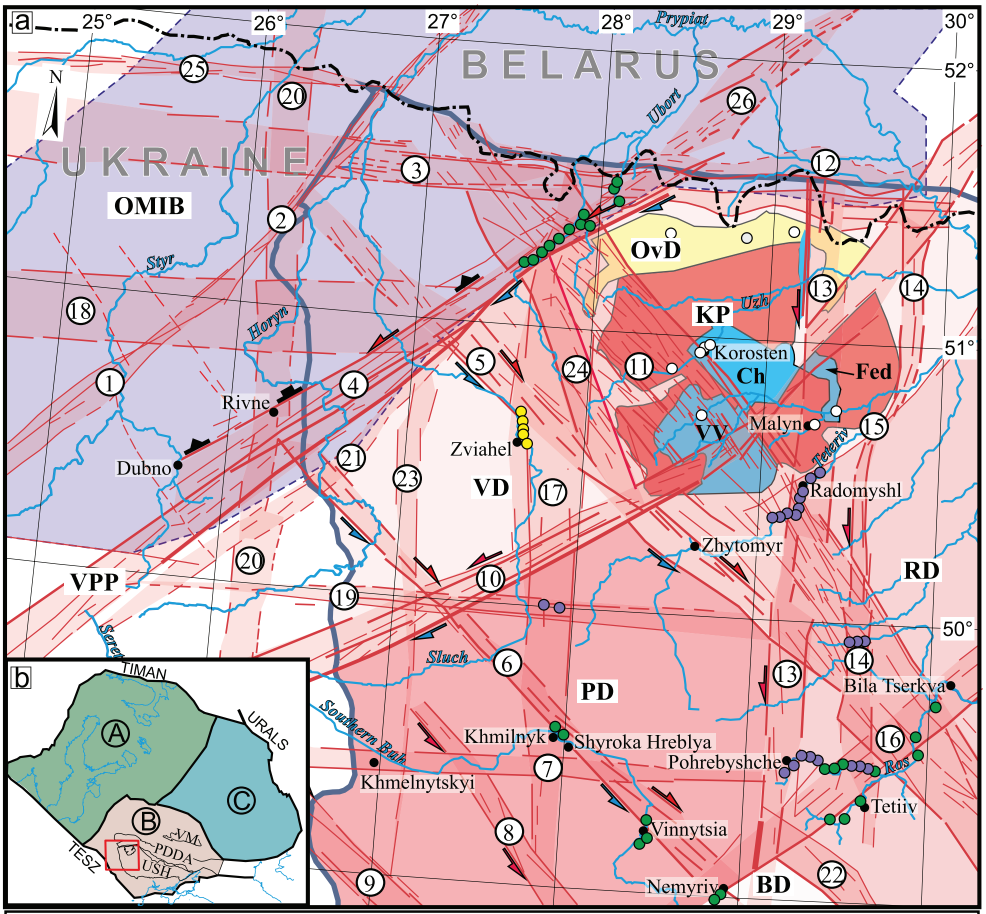

LEGEND

Border of the Ukrainian Shield.

20 Faut zones (numbers in circles): 1 – Lutsk, 2 – Horyn, 3 – Polissia, 4 – Sushchany–Perha, 5 – Sarny–Varvarivka, 6 – Khmilnyk, 7 – Khmelnytskyi, 8 – Letychiv, 9 – Podolian, 10 – Teteriv, 11 – Central, 12 – South-Prypiat, 13 – Zvizdal–Zalissia, 14 – Brusyliv, 15 – Chornobyl, 16 – Nemyriv, 17 – Bilokorovychi, 18 – Volodarsk-Volynskyi, 19 – Andrushivka, 20 – Rivne, 21 – Ostroh, 22 – Dashiv, 23 – Shepetivka, 24 – Yemilchyne, 25 – North-Ratkiv, 26 – Malyn–Symonavichy.

Kinematic markings of fault zones (a – at the time of initiation, b – during the main activation phase):

a b dextral strike-slip fault

a b sinistral strike-slip fault

normal fault (during the main activation phase)

reverse fault (during the main activation phase)

Osnitsk–Mikashevychi Igneous Belt (OMIB).

Points of tectonophysical research. The colour coding indicates the respective faulting stages: yellow – Uman–Novohrad-Volynskyi stage; green – Nemyriv stage; purple – Subottsi–Moshorine stage; white – Korosten stage.

Ukrainian Shield domains: VD — Volyn, PD — Podolian, RD — Ros', BD — Buh. Korosten Pluton (KP) massifs: VV — Volodarsk-Volynskyi, Fed — Fedorivka, Ch — Chopovychi. Superimposed depression: OvD — Ovruch. Regional structures (inset b): TESZ — Trans-European Suture Zone, VM — Voronezh Massif, PDDA — Pripyat–Dnieper–Donets Aulacogen, VPP — Volyn–Podillya Plate.

Fig. 1. Tectonic scheme of the main structural units of the western part of the Ukrainian Shield **(a)** (modified after Krylov 1988; Entin et al. 2002; Entin 2005), and the super-regional elements of the East European Craton **(b)**. Letters in circles: Fennoscandia (A), Sarmatia (B), Volgo-Uralia (C) (Bogdanova et al. 1996; Gintov & Pashkevich 2010). The study area is outlined by the red rectangle.

re-collisional transitional period characterized by the redistribution of stress fields and the kinematics of inter-domain fault systems. The latter evolved as an active continental margin and consisted of a bimodal volcano-plutonic association (Shcherbakov 2005; Shumlyanskyy 2014). Both belts were intruded at 1.80–1.74 Ga by the anorogenic Korosten Pluton, which represents the anorthosite–mangerite–charnockite–granite (AMCG) complex. The causes of this late magmatic phase – coeval with the Subottsi–Moshoryne faulting stage and the Korosten deformation episode – are discussed by Bogdanova et al. (2013) and Shumlyanskyy et al. (2016, 2017). For the Korosten Pluton, an origin related to extensional zones formed during plate reorganization (collision of Fennoscandia with Volgo-Sarmatia) has been proposed. In particular, petrological and mineralogical data from these massifs point to a polybaric crystallization pathway for the Korosten anorthosites, reflecting complex magma evolution at various crustal levels (Mytrokhyn et al. 2008). During the same magmatic phase (1799–1777 Ma), dolerite dyke swarms and layered tholeiitic dolerite intrusions of the Prutivka Complex formed, compositionally like dyke swarms associated with Large Igneous Provinces (Shumlyanskyy et al. 2016). It has also been suggested that these tholeiitic dolerites reflect post-collisional mantle plume activity at 1800–1740 Ma (Shumlyanskyy et al. 2016).

Here we reconstruct the timing and activation stages of fault zones by establishing the chronological and spatial links between tectonic disruption and magmatic activity for 2.05–1.73 Ga. This enables us to trace their impact on the present-day crustal framework, as manifested by density heterogeneity and characteristic features of the regional magnetic field.

Numerous isotopic age constraints from all magmatic complexes within the Volyn Domain make it possible to correlate tectonic and magmatic events and to extend the established dating of faulting stages to the Podolian and Ros' domains.

To reconstruct spatio-temporal relationships between deformation and magmatism in the western part of the USh, we use field-based tectonophysical results from the Sushchany–Perha, Zvizdal–Zalissia, Brusyliv, Nemyriv, and Khmilnyk fault zones, the Novohrad-Volynskyi granitoid massif, and the Korosten Pluton of gabbro–anorthosite and rapakivi granite. We also draw on tectonophysical and structural studies of the Teteriv, Sarny–Varvarivka, Chornobyl, Bilokorovychi, and Podolian fault zones (Gintov & Mychak 2014; Mychak 2014; Mychak et al. 2016, 2022; Gintov et al. 2018; Mychak & Farfuliak 2021).

Key attributes of USh fault zones (Gintov & Mychak 2014) are: (1) widths of 7–25 km with penetration into the mantle to several tens to a few hundred kilometres; (2) early Proterozoic ages, less commonly Neoarchaean; (3) regardless of whether formed under compression or extension, they are permeable to solutions and fluids owing to dilatant loosening of rocks; (4) nearly all zones experienced multiple reactivations up to the present; (5) displacements on fault walls are often reversed between activation phases, i.e., strike-slip faults can switch between sinistral strike-slip fault and dextral strike-slip fault movement.

Research methods

Stress-field investigations within Precambrian crystalline shields have also been actively conducted in other regions of the world. In particular, the stress state and palaeostress evolution of the crystalline basement have been studied in detail within the Canadian Shield based on stress measurements and analysis of brittle structures (Zoback & Zoback 1989; Zang & Stephansson 2010), the Fennoscandian Shield with consideration of postglacial and present-day tectonic stresses (Lund & Zoback 1999; Heidbach et al. 2010), as well as within the Siberian Craton and other intracratonic domains (Delvaux et al. 1997). Beyond classical stress-field reconstructions, recent structural and analogue modelling studies have further illuminated deformation patterns and stress transfer mechanisms in intraplate settings, including the role of antithetic faults in deformation relay zones (Cammani et al. 2023) and analogue modelling of intraplate strike-slip tectonics providing new insights into stress localization and transfer (Dooley & Schreurs 2012). The obtained results indicate a complex spatial and temporal evolution of stress regimes in the crystalline crust, highlighting the importance of comparative studies, particularly for the USh, in understanding the general patterns of its tectonic evolution.

To analyse the internal structure of fault zones in the western part of the USh, we conducted detailed mapping and measurements of secondary structural–textural elements, including banding, lineation, schistosity, cleavage, and fracture systems. In actively deforming zones – especially strike-slip fault zones – fractures do not form randomly, but develop a regular geometry dictated by the prevailing stress field. Domains in which deformation is localized into linear structures are termed shear-fracture zones, which at a larger scale manifest as brittle faults.

Fractures within these zones form well-defined structural parageneses – spatially ordered sets of brittle structures (Fig. 2) — that develop during a single tectonic stage and reflect a common stress–strain regime. Characteristic fracture types within shear-fracture zones, together with their mutual orientation and kinematic indicators, were used to reconstruct the stress–strain state during relatively late deformation episodes. Shear-fracture zones often also contain S-shaped elements (F-structures) formed by combined shear and compression, which provide important constraints on deformation mechanisms and sense of movement.

Field data were processed and interpreted using structural-paragenetic and kinematic methods of tectonophysics (Gintov 2005), including careful measurement of fracture strike azimuths and dips. Statistical analysis of structural orientations was performed using stereographic projection with the Stereonet software package (Allmendinger et al. 2012).

The structural-paragenetic method identifies spatial relationships and the sequence of fracture formation. It delineates elements that formed within a single stress field, in which the principal stress axes (σ_1 – maximum compression; σ_2 – intermediate; σ_3 – extension) maintained stable orientations, thereby establishing a relative chronology of deformation events.

The kinematic method is based on the analysis of fault mirrors and slickenside striations that record the sense and direction of strike-slip fault motion. These features constrain the orientation of the most recent stress field active during the latest reactivation.

Joint application of both methods provides a multifactor approach to reconstructing the tectonic history of the USh, allowing the sequence, duration, and conditions of deformation stages to be defined.

Based on the 3D gravity modelling results by GMT-Auto program (Makarenko et al. 2021, 2023) on a 10×10 km we show the density distributions at depths of 5, 10, 20 km, and Moho, and we examine a depth behaviour of the studied fault zones in the crust. The gravity date for the modelling were taken from the map of complete Bouguer anomalies (Scheme of gravity field of Ukraine 2002).

We also confronted our results with results of magnetic field interpretation. Using 3D magnetic modelling by (Kovalenko-Zavoysky & Ivashchenko 2006) the magnetic properties of the lower crust were as estimated, and extensive mafic dykes and dyke swarms representing — usually significant magnetic sources were analyzed, as they help us in studying the origin of mantle and recording mantle and lower-crustal melt provenance (Pashkevich et al. 2006; Mychak et al. 2023).

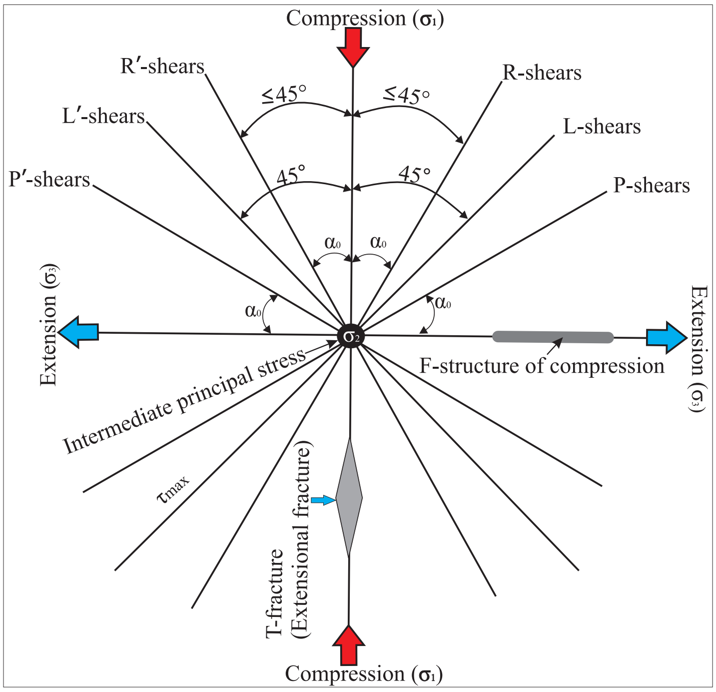

Fig. 2. Schematic arrangement of principal stress axes and second-order structures at the time of their formation. Explanatory notes: R – Riedel shears (~15–30° to the principal shear direction); R′ – conjugate Riedel shears (at a larger angle, >45°); L – shear fractures oriented parallel to the shear direction; P – shears oriented symmetrically to R-shears relative to the shear direction; T-fracture – extensional fractures perpendicular to σ_3. S-shaped elements (*F-structures*) indicate combined shear and compression (transpression). σ_1, σ_2, σ_3 – principal compressive, intermediate, and tensile stress axes, respectively. Structural-paragenetic interpretation following (Gintov 2005; Cammani et al. 2023).

Results and discussion

In chronological order we distinguish four deformation stages in the western USh; their kinematic characteristics are summarized in Table 1. Magmatic complexes are grouped by age and correlated with deformation stages (Table 2).

Uman–Novohrad-Volynskyi deformation stage (2.08–2.00 Ga)

During the pre-collisional transitional period, intensive transtensional granite formation took place. This deformation stage was first distinguished based on detailed tectonophysical investigations of the coeval Novohrad-Volynskyi (Volyn Domain), Uman (Ros' and Buh domain), and Novoukrainskyi (Inhul Domain) granitoid massifs of the Ukrainian Shield (Mychak 2014). In the Volyn Domain of the USh, this deformation stage accompanied with autochthonous and intrusive granites of the Zhytomyr and Sheremetiv complexes (Shcherbakov 2005; Shcherbak et al. 2008; Shumlyanskyy et al. 2018; Usenko 2024) (Fig. 3, Table 2).

The granites and migmatites of the Berdychiv (within the Podolian Domain) and Zvenyhorodka (within the Ros' Domain) complexes were formed during the orogenic stage. The Berdychiv granites originated in four major episodes: 2220–2150 Ma, 2090–2080 Ma, ca. 2040 Ma, and 2000 –1930 Ma, while the formation of the Zvenyhorodka complex is dated at 2139–2032 Ma (Shcherbakov 2005; Shcherbak et al. 2008; Stepaniuk et al 2015).

The northern part of the Novohrad-Volynskyi Massif (represented by the granitoids of the Zhytomyr Complex) is composed predominantly of medium-grained grey granites with porphyritic K-feldspar phenocrysts (Fig. 4a). Toward the central part of the massif, the granites become more melanocratic; near Zviahel, on both banks of the Sluch River, they exhibit a well-developed trachytoid texture (Fig. 4b). During the tectonophysical investigation of biotite granites of this complex, systematic measurements were carried out on the orientations of brittle fractures and the trachytoid fabric. The investigated trachytoid texture, acting as a primary magmatic lineation, records deformation processes synchronous with and immediately following magma emplacement. This is evidenced by the orientation and rotation of prismatic K-feldspar crystals (1–10 cm in size) forming flow structures along shear

Table 1: Kinematic characteristics of the faults and intrusive massifs 2.05–1.73 Ga in the Ukrainian Shield (Gintov 2005; Gintov & Mychak 2014; Mychak 2014; Mychak et. al. 2016, 2022, 2023; Mychak & Farfuliak 2021).

Age, Ga	Stage of deformation	Fault zones	Fault characteristics during their initiations or reactivations					Orientation of the principal stress axes				Phase of faulting				
								formation		activation						
			Length (km)	Width (km)	Strike (°)	Dip (°)	Kinematics	σ_1 (°)	σ_3 (°)	σ_1 (°)	σ_3 (°)	Shear zone	σ_1 (°)	σ_3 (°)	σ_2 (°)	Kinematics
1.80–1.73	Korosten	Korosten Pluton	WE – 150 NS – 110	12 000 km^2			Extentional	333/0	63/0							
1.85–1.73	Subottsi–Moshorine	Brusyliv	160	15	360	90	Dextral*	314/0	44/0			Brusyliv	314/00	44/00	180/80	Dextral
		Zvizdal–Zalissia	350	8	360	90	Dextral	315/0	45/0	100/85	280/05	Zvizdal 1	315/00	45/00		Sinistral
												Zvizdal 2	45/00	315/00		Dextral
												Dyke formation	110/85	280/05	10/02	Normal fault
1.99	Nemyriv	Nemyriv	285	13	50	90	Sinistral**	185/0	95/0	85/0	355/0	Nemyriv	185/05	95/05	320/84	Sinistral
												Suchany	85/04	175/05	310/85	Dextral
												Rogozny	120/05	210/05	350/85	Dextral
		Teteriv	140	12	46	90		Not tectonophysically studied								
		Sushchany–Perha	200	10	50	85 NW	Sinistral	185/0	95/0	85/0	355/0	Khmelivka	185/02	95/02	330/88	Sinistral
												Suchany	85/05	355/05	220/05	Dextral
												Perha 1	286/20	12/20	150/70	Dextral
												Perha 2	335/05	140/85	240/02	Thrust
												Rudnia–Khochynska	150/78	342/12	246/02	Normal fault
												Lopatychi	300/07	30/02,	135/83	Dextral
		Chornobyl	110	6	38	85 SE	Sinistral	185/0	95/0	85/0	355/0					
		Sarny–Varvarivka	260	10	305	85 SW	Dextral	170/0	260/0	170/0	260/0					
		Khmilnyk	350	8	318	90	Dextral	03/00	93/00	85/00	355/00	Nemyriv	03/00	93/00		Dextral
												Suchany	85/00	355/00		Sinistral
		Podolian	210	12	309	90	Dextral	03/00	93/00	85/00	355/00					
2.05–2.04	Uman–Novohrad – Volynskyi	Novohrad-Volynskyi massif					Dextral and extensional	301/00	31/00							

* Dextral strike-slip fault; ** Sinistral strike-slip fault

Table 2: Expression of deformation stages in magmatism (Volyn Domain).

Age, Ma	Complex name	Location	Reference
	Korosten deformation and magmatic stage		
Main phase of the Korosten Pluton			
1743±5	Rare-metal granite	Korosten Pluton	Shumlyanskyy et. al. (2017)
1761±13	Rhyolite	Ovruch Basin	
1758±1.8 1760.6±0.7 1756±5 1761±4 1756±4 1771.5±0.8 1763±8 1761±4	Main anorthosite Pegmatite Olivine monzodiorite Monzodiorite Main anorthosite Gabbronorite	Volodarsk-Volynskyi Massif Fedorivka Massif Korosten Pluton	
1765±5 1765±3	Granite	Korosten Pluton	
1772±6	Syenite	Yastrebetsky Massif	
Dyke generation II			
1760.7±1.7	Plagiophyric ferromonzodiorite dyke	Pugachivka dyke	Shumlyanskyy et. al. (2017)
1751±12	Ferromonzodiorite sill	Bondary sill	
1758.8±0.9 1761.9±1.6 1764±3	Olivine gabbro Monzodiorite Syenite	Buky Massif	Shcherbak et al. (2008), Shumlyanskyy et. al. (2017)
Early phase of the Korosten Pluton			
1817±15 1810±14 1780±6	Granite	Northern part of the Korosten Pluton	Shumlyanskyy et. al. (2017)
1781±8 1784±3 1789±2	Early anorthosite	Fedorivka Massif Chopovychi Massif	
1789±1.5	Gabbro	Davydky Massif	
Dyke generation I			
1789±9	Ferromonzodiorite dyke	Zamyslovychi dyke	Shumlyanskyy et. al. (2017)
1793±3	Ferromonzodiorite dyke	Rudnya–Bazarska dyke	
1799±10	Ferromonzodiorite dyke	Bilokorovychi dyke	
Prutivka tholeiitic dolerite complex			
1777±4.7	Dolerite	Prutivka sill-like intrusion	Shcherbak et al. (2008), Shumlyansky et. al. (2016)
1787±6.4 1791±5	Dolerite	Tomashhorod dyke	Shumlyansky et. al. (2016)
1788 1790	Gabbro	Kamyanka Massif	
	Subottsi–Moshoryne deformation stage		
Up to 1800	Sandstones, Metabasalts	Bilokorovychi Depression	Shumlyansky et. al. (2016)
	Nemyriv deformation stage		
Osnytsk–Mikashevychi igneous belt			
1993.8±3.2 1996±13	Granite Rhyolite	Osnytsk complex Klesiv group	Shcherbak et al. (2008) Shumlyansky (2014)
Gabbronorite–monzonite Buky Complex			
1987±5.8	Gabbro Granite	Buky Massif	Shcherbak et al. (2008)
1992±5	Gabbronorite Granite	Zhybrovychi Massif Kyshyn Massif	
2014±15	Mafic and ultramafic alkaline rocks	Horodnytsya Complex	Shumlyansky et. al. (2016)
	Uman–Novohrad-Volynskyi deformation stage		
2045 2060 2072 2078	Granite	Zhytomyr Complex intruded during several successive phases	Shumlyansky et. al. (2018)
2078 2092	Plagiogranites	Sheremetiv Complex intruded during several successive phases	
2028±12 2044±9 2059±5 2083±9	Granite	Novohrad–Volynskyi Massif	

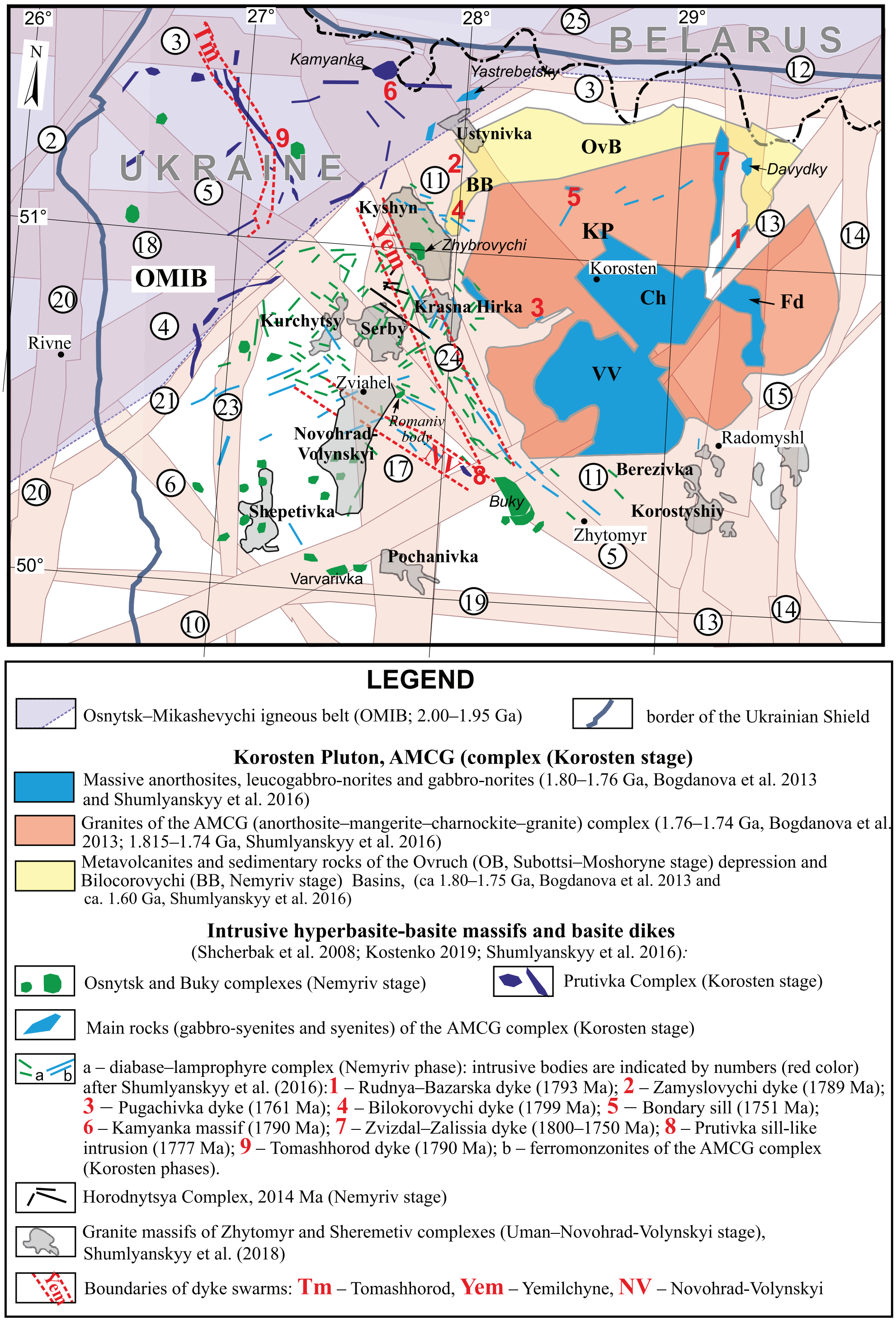

Fig. 3. Schematic geological map of the intrusive massifs and dykes in the Volyn Domain (Northwestern of the Ukrainian Shield), modified after Shcherbak et al. (2008), Bogdanova et al. (2013), Shumlyanskyy et al. (2016, 2017), Kostenko (2019).

fractures. The spatial distribution of this magmatic lineation is fully consistent with the local and regional transtensional stress field.

Most measured fractures (approximately 90 %) are steeply dipping, with inclinations ranging from 65° to 90°, whereas gently dipping fractures (<65°) account for only about 10 %. Analysis of strike azimuths of subvertical shear fractures reveals four pronounced maxima at 69° (A), 94° (B), 306° (C), and 332° (D) (Fig. 4c). Maxima B and D are interpreted as Riedel (R) shears, typical of strike-slip fault deformation. Maximum C corresponds to tensile fractures formed under extensional conditions, whereas maximum A is associated with L′-type shear fractures, also characteristic of strike-slip systems.

Kinematic analysis of the fracture network allowed reconstruction of the principal stress axes. The subhorizontal maximum compressive stress axis (σ_1), derived from the orientations of R, R′, and L′ shears, has calculated azimuths of 305° and 297°, yielding a mean value of 301°. Accordingly, the extension axis (σ_3) is oriented at 31°, indicating a dextral strike-slip regime with a significant extensional component. This stress configuration is consistent with tectonophysical evidence for granite emplacement under a regional strike-slip–extension stress field (σ_1=301°, σ_3=31°). The tectonophysical evidence for granite emplacement under these conditions is primarily represented by the established parageneses of high-temperature cooling fractures with characteristic shear angles of α_0=25–35° (Mychak 2014), which formed extensively during the crystallization and syncrystalline cooling of the granitoids. Our findings indicate that this reconstructed transtensional stress field was not a local feature restricted to the Novohrad-Volynskyi Massif, as an identical stress regime was synchronously recorded within the Uman Massif (Ros' and Buh domains). This regional tectonic regime facilitated the widespread development of transtensional structural pathways that enabled magma ascent prior to the final collisional consolidation of the shield domains.

Geochronological dates indicate that the granite massifs of the Zhytomyr and Sheremetiv complexes were formed in 2083, 2059, 2044, and 2028 Ma (Shumlyanskyy et al. 2018).

Nemyriv deformation stage (1.99 Ga)

The OMIB formed as an active continental margin developed on the Zhytomyr–Teteriv basement in response to oceanic plate subduction at ca. 2000–1980 Ma (Shumlyanskyy 2014; Stepanyuk et al. 2020; Usenko 2025). These tectonomagmatic processes correspond to the Nemyriv faulting stage. This stage produced diagonal sinistral strike-slip faults of NE trend (Nemyriv, Teteriv, Sushchany–Perha, Chornobyl fault zones) and dextral strike-slip faults of SW trend (Sarny–Varvarivka, Khmilnyk, and Podolian zones).

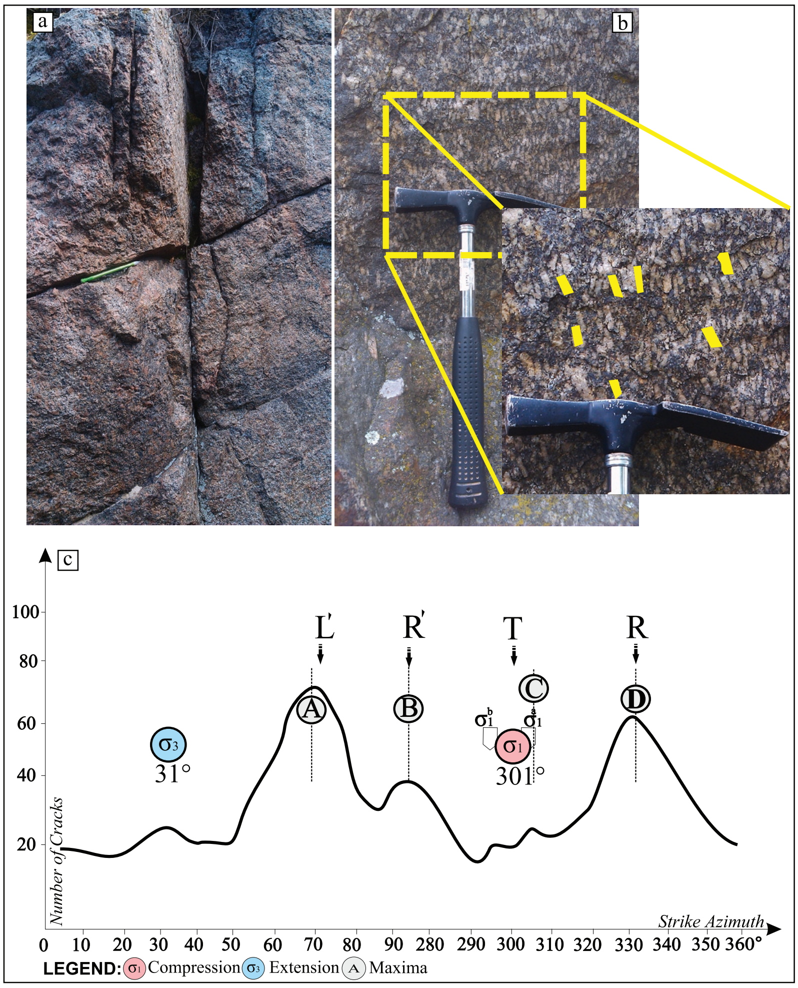

Fig. 4. The results of tectonophysical studies of the Novohrad-Volynskyi granitoid massif: **(a)** fracturing in the granites of the Zhytomyr complex; **(b)** trachytoid texture in the granites of the Zhytomyr complex; **(c)** total graph of azimuths of stretches (> 65°) deeply falling cracks in the Novohrad-Volynsk granitoid massif. Photo by S.V. Mychak.

Within the USh, the OMIB is bounded by the Sushchany–Perha fault zone to the southeast and the South-Prypiat fault zone to the north. The OMIB comprises metabasalt and andesite–dacite–rhyolite associations of the Klesiv Series, which are metamorphosed from greenschist to low-amphibolite facies, together with their intrusive counterparts represented by the gabbro–diorite–granodiorite –monzogranite association of the Osnytsk Complex (see Fig. 3, Table 2). Mantle-derived melts from which crystallize metabasalts, metaandesite-basalts, and amphibolitized dolerites are preferentially associated with the diagonal fault, whereas crustal-derived Osnytsk granites are linked to sub-latitudinal and ENE-trending zones (Shcherbakov 2005). Isotopic signatures (positive εNd values and low initial $^{87}Sr/^{86}Sr$ ratios) indicate mantle sources for the primary mafic melts, whereas geochemical data suggest formation in a subduction-related setting, i.e., an active continental margin for the OMIB (Shumlyanskyy 2014). Relationships between granites and mafic rocks attest to repeated inputs of melts from both mantle (basaltic) and crustal (granitic) partial-melting reservoirs (Usenko 2025).

Intrusions of the Buky Complex (formed at ca. 2.0–1.95 Ga; see Stepanyuk et al. 2020; Vysotsky et al. 2020) also formed during the Nemyriv faulting stage. The complex is localized at the intersection node of the Teteriv and Sarny–Varvarivka fault zones, which separate

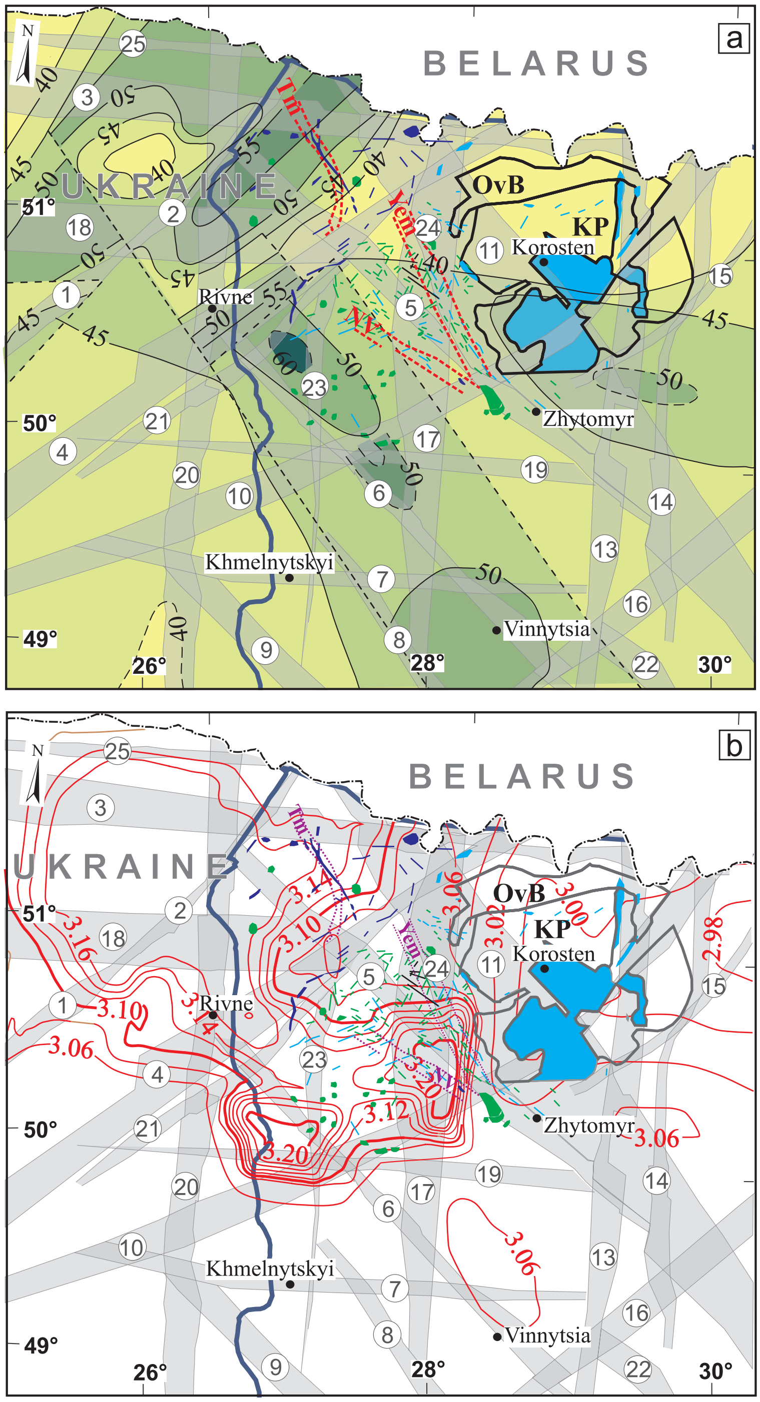

Fig. 5. Moho depth **(a)** in km and density at the Moho **(b)** in (g cm⁻³). Dashed line in (a) indicates surface projections of zones with abrupt Moho offsets. Other legend symbols as in Figs. 1, 3.

the Volyn and Podolian domains (see Figs. 1, 3). It comprises a diverse gabbro–diorite–granodiorite–granite rock association, representing a mixture of mantle-derived mafic–ultramafic and crustal intermediate-to-felsic magmas (Usenko 2025). Their many similarities to the Osnytsk Complex may indicate a common melt source (Shcherbakov 2005). The Buky Complex formed away from the OMIB in a convergent geodynamic setting (Shumlyanskyy 2012, 2014; Stepanyuk et al. 2020). Several Osnytsk and Buky intrusions are concentrated within the Volyn Domain, which is bounded by the sinistral strike-slip faults of NE strike (Sushchany–Perha and Teteriv fault zones) and by the Rivne and Bilokorovychi meridional fault zones. This domain exhibits a greater crustal thickness (Fig. 5a), which changes from 40 km up to more than 60 km and higher densities at the Moho (3.14–3.20 g cm^{-3}, (Fig. 5b). The Buky (1987 Ma) Massif sits at the intersection of the Teteriv and Sarny–Varvarivka fault zones; the Varvarivka Massif lies at the intersection of the Khmilnyk and Teteriv fault zones (Fig. 3). The Zhubrovychi subvolcanic body (1992 Ma; Shcherbak et al. 2008), composed of gabbro-norites, along with the Romaniv gabbroid body within the Novohrad-Volynskyi Massif, are also confined to these deep-seated fault intersections. Their localization and composition indicate that mantle-derived mafic melt sources actively operated during this stage alongside crustal reservoirs (Usenko 2025). Alkaline ultramafic bodies of the Horodnytsya Complex (2014 Ma; Shumlyanskyy et al. 2016) likely formed at the intersection of the Sarny–Varvarivka, Yemilchyne, and Central fault zones at the beginning of the Nemyriv stage. The complex is represented by a system of dykes and small hypabyssal intrusions composed predominantly of olivine melteigites, olivine jacupirangites, and their dyke analogues (Kryvdik et al. 2003). The melt generation depths for these alkaline ultramafics are comparable to those of kimberlites, i.e., depth >200 km (Shcherbakov 2005; Usenko 2025).

The Kyshyn and Ustynivka massifs represent late magmatic expressions linked to the evolution of the Osnytsk Magmatic Belt, being younger than the main phase of the Zhytomyr Complex granites (Shumlyanskyy et al. 2018; Usenko 2024). The Kyshyn Massif is a complex central-type volcano-plutonic structure. The former is located at the northern contact between the Yemilchyne and Sarny–Varvarivka fault zones; the latter sits at the intersection of the Sushchany–Perha and Central fault zones (see Fig. 3). The principal lithologies of the Kyshyn Massif include dacite–rhyolite and andesite–basalt volcanic rocks with associated tuffs, which are intruded by granitoids of two distinct age groups at ca. 2.05 Ga and ca. 1.92 Ga, as well as syenites dated at ca. 1.96 Ga. The Ustynivka Massif is composed predominantly of granitoids that are petrogeochemically similar to the Zhytomyr Complex but chronologically younger, with ages shifting toward 1975–1955 Ma (Kostenko 2019; Shumlyanskyy et al. 2018).

Diabase–lamprophyre dykes of the Osnytsk Complex were emplaced within the Volyn Domain during the Nemyriv stage (Kostenko 2019). The Novohrad-Volynskyi and Yemilchyne dyke swarms are localized within a crustal block bounded by the Sushchany–Perha, Teteriv, and Rivne fault zones. Among them, the Novohrad-Volynskyi swarm is the largest; it trends NW with a strike azimuth of 310–320° and is structurally linked to the Sarny–Varvarivka fault zone, which was reactivated in the Late Proterozoic as a sinistral strike-slip fault (Pashkevich et al. 2006; Mychak et al. 2023). The Yemilchyne swarm, characterized by a strike azimuth of 330–335°, follows the corresponding NW-trending fault zone (see Fig. 3).

Sushchany–Perha fault zone

The Sushchany–Perha fault zone bounds from the south the OMIB, juxtaposes the Zhytomyr and Osnytsk granitoids, and deforms them predominantly as a sinistral strike-slip fault. At the same time, it flexes the Tomashhorod dyke (1791–1787 Ma; Shumlyanskyy et al. 2016) with a dextral strike-slip sense (Fig. 3), indicating repeated reactivation of the fault system under changing stress regimes. The principal field observation points and structurally studied localities within these magmatic complexes are mapped in Figure 1. Fracture and structural–textural analyses reveal five main stages (six phases) of faulting (Fig. 6, Table 1), each characterized by the development of shear-fracture belts with distinct orientations, with more detailed background information provided in Mychak & Farfuliak (2021). The evolution of the Sushchany–Perha fault zone occurred through several deformation phases, the relative ages of which were established based on the vergence relationships of L- and R-shears. In decreasing order of age, the following phases were identified. The Khmelivka phase is characterized by σ_1=185°/02°, σ_3=95°/02°, and σ_2=330°/88°, corresponding to a sinistral strike-slip regime. This was followed by the Sushchany phase (σ_1=85°/05°, σ_3=355°/05°, σ_2=220°/85°), marked by dextral strike-slip deformation. Together, the Khmelivka and Sushchany phases are associated with the formation of the Nemyriv and Khmilnyk fault zones; and both phases deform the granitoids of the Osnytsk and Zhytomyr complexes.

Subsequent deformation is represented by the Perha phase, subdivided into two subphases. Perha-1 is defined by σ_1=286°/20°, σ_3=12°/20°, and σ_2=150°/70°, whereas Perha-2 reflects a thrust regime with σ_1=335°/05°, σ_3=140°/85°, and σ_2=240°/02°. These were followed by the Rudnia–Khochyn phase (σ_1=150°/78°, σ_3=342°/12°, σ_2=246°/02°), characterized by normal faulting, and finally by the Lopatychi phase, which records renewed dextral strike-slip deformation (σ_1=300°/08°, σ_3=30°/02°, σ_2=135°/83°). The Perha and Rudnia–Khochyn phases reflect heightened tectonic activity related to oblique collision and interaction between Fennoscandia and Sarmatia, producing alternating compressional and extensional stress fields. Normal- and reverse-fault stress fields are particularly associated with NW–SE compression during this collisional stage.

In the 3D density model (Fig. 7), the Sushchany–Perha fault zone is expressed throughout the crustal section. In horizontal density slices at depths of 5 and 10 km (Fig. 7a, b), this fault zone is manifested by considerable density horizontal gradients, local anomalies of small wavelength, and sigmoidal bends of density isolines. In a slice of 20 km depth (Fig. 7c) and on Moho, its manifestation disappearing SW from of the city Rivne. Based on a detailed analysis of this fault zone's features in different density slices, we can assume that it dips to the NW.

The intersection of the Sushchany–Perha and Central fault zones is represented by significant horizontal density gradients at depths of 5 and 20 km (Fig. 7a, b) and a density of approximately 3.07 g cm^{-3} at the Moho. In the easternmost part of the section, between the Polissia and Sushchany–Perha fault zones (horizontal density slices at 5 and 10 km, Fig. 7a, b), anomalously high densities (2.80–2.88 g cm^{-3}) can be observed, while in the horizontal Moho slice, the density increases NW-ward from 3.09 to 3.17 g cm^{-3}.

Khmilnyk fault zone

Near Khmilnyk, the crystalline basement records a progressive transition from charnockites dated at ca. 2.22 Ga through garnet migmatites containing charnockite inclusions to garnet–biotite rocks and Berdychiv granites (Shcherbakov 2005; Shcherbak et al. 2008). These lithologies are strongly affected by deformation related to the Khmilnyk fault zone. Fractures and compositional banding predominantly strike NW (azimuth 310–330°) and dip steeply (80–90°) to the NE (Fig. 8a). In a quarry near Shyroka Hreblya, these garnet–biotite porphyroblastic granites and migmatites of the Berdychiv Complex (Stepanyuk 2024) are cut by a ~30 m-thick gabbro–diabase dyke striking 310° (Fig. 8b), indicating syn- to post-deformational mafic intrusion. Mylonitic banding also shows a dominant NW strike (310–320°) with steep NE dips (80–90°), consistent with intense ductile–brittle shearing.

Kinematic analysis reveals well-developed systems of L- and R-shears expressed by mylonites. The dominant shear sets (L: 48/85°; R: 63/87°) indicate dextral strike-slip faulting with a subhorizontal shear component, whereas locally developed younger shear systems (L: 40/85°; R: 23/90°) record subsequent sinistral strike-slip reactivation. Reconstruction of the principal stress axes allows discrimination of two main deformation phases affecting the Khmilnyk fault zone. The Nemyriv phase, corresponding to the Nemyriv fault zone, is characterized by σ_1 oriented at 03°/00° and σ_3 at 93°/00°, with a vertical σ_2 axis, reflecting dextral strike-slip deformation. This was followed by the Sushchany phase, related to the Sushchany–Perha fault zone, with σ_1=85°/00°, σ_3=355°/00°, and vertical σ_2, indicating sinistral strike-slip faulting.

The observed structural orientations and kinematic indicators (Fig. 8c, Table 1) collectively record deformation during the Nemyriv stage, linking the Khmilnyk fault zone to the broader Nemyriv and Sushchany–Perha tectonic evolution.

This structural framework is further refined by precise geochronological data from the area. Specifically, U–Pb monazite dating of the Shyroka Hreblya quarry granite yields 2039±4.8 Ma (Stepanyuk 2024), providing a temporal marker for the magmatic activity associated with these tectonic processes.

In horizontal slices of the 3D gravity model (Fig. 7a, b, c), the densities within the Khmilnyk zone increase south-eastward. In a slice of 5 km (Fig. 7a) the densities are 2.70–2.82 g cm^{-3}, 2.76–2.84 g cm^{-3} (10 km, Fig. 7b), and 2.80–2.88 g cm^{-3} (20 km, Fig. 7c). In the slice of Moho depth (Fig. 5b), a high-densities (3.14–3.20 g cm^{-3}) occur in the region bounded the Teteriv, Ostroh, Rivne and Sarny–Varvarivka fault zones, while in SE direction from this zone the densities are lower (3.06 g cm^{-3}) (Fig. 5b).

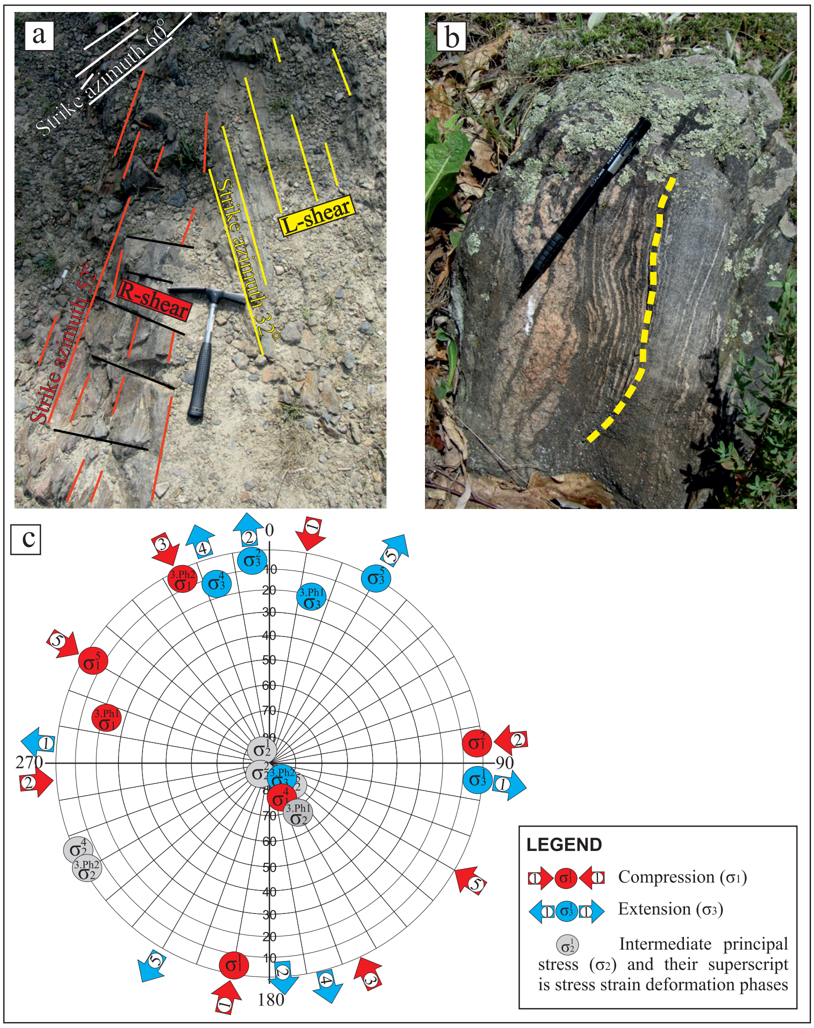

Fig. 6. Results of tectonophysical studies of the Sushchano–Perga fault zone: **(a)** tectonic delamination of granitoids of the Osnytsk Complex; **(b)** migmatite zonation in granitoids of the Zhytomyr Complex; **(c)** results of the inverse kinematic task for the Sushchany-Perha fault zone. Photo by S.V. Mychak.

Nemyriv fault zone

This NE-trending zone intersects the meridional Zvizdal–Zalissia zone, then crosses the Ros' Domain of the USh as an intra-block fault and partly marks the boundary between the Podolian and Buh domains (Fig. 1). Fracture measurements near the Pohrebyshche intersection identify stress fields of the Subottsi–Moshoryne faulting stage (Zvizdal–Zalissia fault zone) and a field with σ_1=05°, σ_3=275° attributed to Nemyriv-zone reactivation. The latter formed under sub-latitudinal compression and sub-meridional extension, whereas initial faulting occurred under sub-meridional compression and sub-latitudinal extension (Gintov 2005). Deformation phases assigned to the Nemyriv zone are listed in Table 1.

Based on the horizontal density slices of the resultant 3D density model we can see that density increasing to the SW along the Nemyriv zone: 2.76–2.80 g cm^{-3} (5 km, Fig. 7a), 2.78–2.84 g cm^{-3} (10 km, Fig. 7b), 2.84–2.88 g cm^{-3} (20 km, Fig. 7c), and 3.06 g cm^{-3} on average at the Moho depth (Fig. 5b).Thus, the structural, magmatic, and geophysical evidence presented in this study allows the tectonic processes of the Nemyriv deformation stage (1.99 Ga) to be integrated into a single coherent tectonic model. This stage corresponds to a transitional convergent–collisional regime that evolved under conditions of regional sub-meridional compression. This compression led to the development of a well-defined conjugate strike-slip fault system consisting of left-lateral northeast-trending fault zones (Nemyriv, Teteriv, and Sushchany–Perga zones) and right-lateral northwest-trending fault zones (Khmilnyk and Podolian zones). Local transtensional and transpressional domains that formed at the intersections of these fault systems created pathways for the ascent of synchronous mantle-derived and crustal melts associated with the Osnytsk and Buky complexes. Our 3D density modelling data clearly record this tectonic stage within the present-day lithospheric structure through pronounced block-related variations in Moho depth (up to 60 km) and elevated densities at the base of the crust (3.14–3.20 g cm^{-3}).

Subottsi–Moshoryne deformation stage (1.85–1.73 Ga)

The subsequent interval (1.85–1.73 Ga) marks the completion of USh assembly and large-scale deformation. Tectonophysical data define two final major deformation stages for this period. During the first of these, the Subottsi–Moshoryne stage, E–W (Polissia, Volodarsk-Volynskyi) and meridional (Zvizdal–Zalissia, Brusyliv, Bilokorovychi) fault

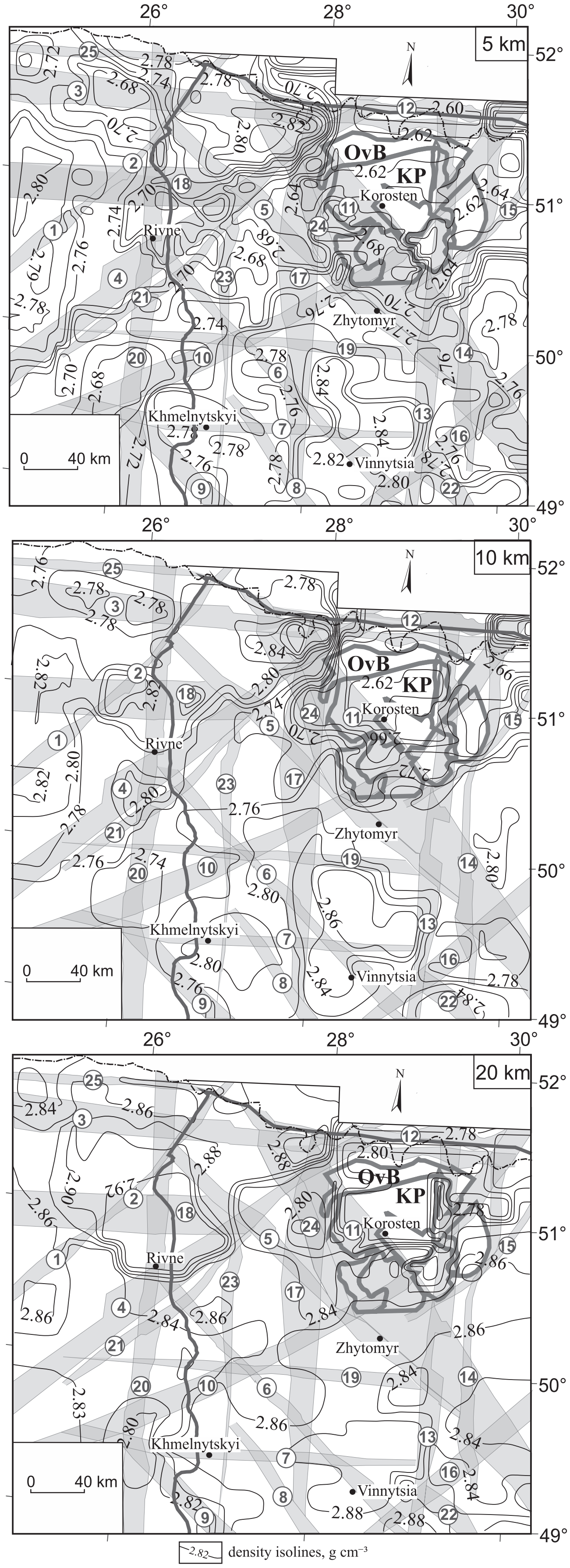

Fig. 7. Density distribution scheme at a depth of 5, 10, 20 km (g cm^{-3}). For other legends see Fig. 1.

zones formed in the NW USh. Deformation occurred under a regional stress field with subhorizontal principal axes σ_1=315° and σ_3=45°, dominated by extensional tectonics. A notable trait of these faults is their pronounced straightness, clearly expressed in magnetic anomalies and density patterns. All mentioned fault zones are readable in our 3D density model (Figs. 7 and 5b) and regional magnetic field map (Fig. 11). On horizontal density slices at depths of 5 km (Fig. 7a), 10 km (Fig. 7b), 20 km (Fig. 7c), Moho (Fig. 5a) and regional magnetic map, they are manifested by horizontal density gradients and gradients of magnetic field as well as sigmoidal changes in isolines of density and magnetic field and anomalies of very small wavelength. The most prominent density (gravity) features characterize the Polissi a and Bilokorovychi fault zones, while the manifestation of the Zvizdal–Zalissia and Brusyliv fault zones disappears with crustal depths. On the map of the magnetic field, the most visible are Volodarsk-Volynskyi and Bilokorovych fault zones. This straightness implies that after this stage the USh did not experience strong deformation capable of reorienting or bending these fault zones (Gintov & Mychak 2014).

Zvizdal–Zalissia fault zone

Tectonophysical analysis of the Zvizdal–Zalissia fault zone reveals three main phases of faulting characterized by differently oriented shear belts, the relative ages of which were determined from the vergence relationships of L- and R-shears. The first two phases are dominated by strike-slip deformation under alternating sublatitudinal and submeridional compression regimes. These phases are characterized by subhorizontal principal stress axes with σ_1 oriented at 315° and σ_3 at 45°, corresponding to the Subottsi–Moshoryne faulting stage. Their timing is close to the emplacement of the Korosten Pluton, as indicated by numerous diagonal veins composed of rapakivi-like Korosten granites south of Radomyshl. In particular, exposures of the crystalline basement occur on the southern outskirts of the village of Marianivka, located south of Radomyshl along the Teteriv River. These exposures are represented by plagiogneisses of the Paleoproterozoic Teteriv Series *(*Shumlyanskyy 2012*)*.

The third deformation phase is marked by a transition to a normal fault regime recorded by fracture systems and biotite gneiss banding (Fig. 9, Table 1). This stress field is characterized by σ_1=100°/85°, σ_3=280°/05°, and σ_2=10°/02°, indicating steeply inclined compression and subhorizontal extension. This extensional regime controlled the emplacement of the Zvizdal–Zalissia mafic dyke (Fig. 3), which is composed of gabbro-dolerites (Shcherbakov 2005; Mytrokhyn & Omelchenko 2006; Shumlyanskyy et al. 2018). This dyke intrudes along the fault zone and exhibits variable but

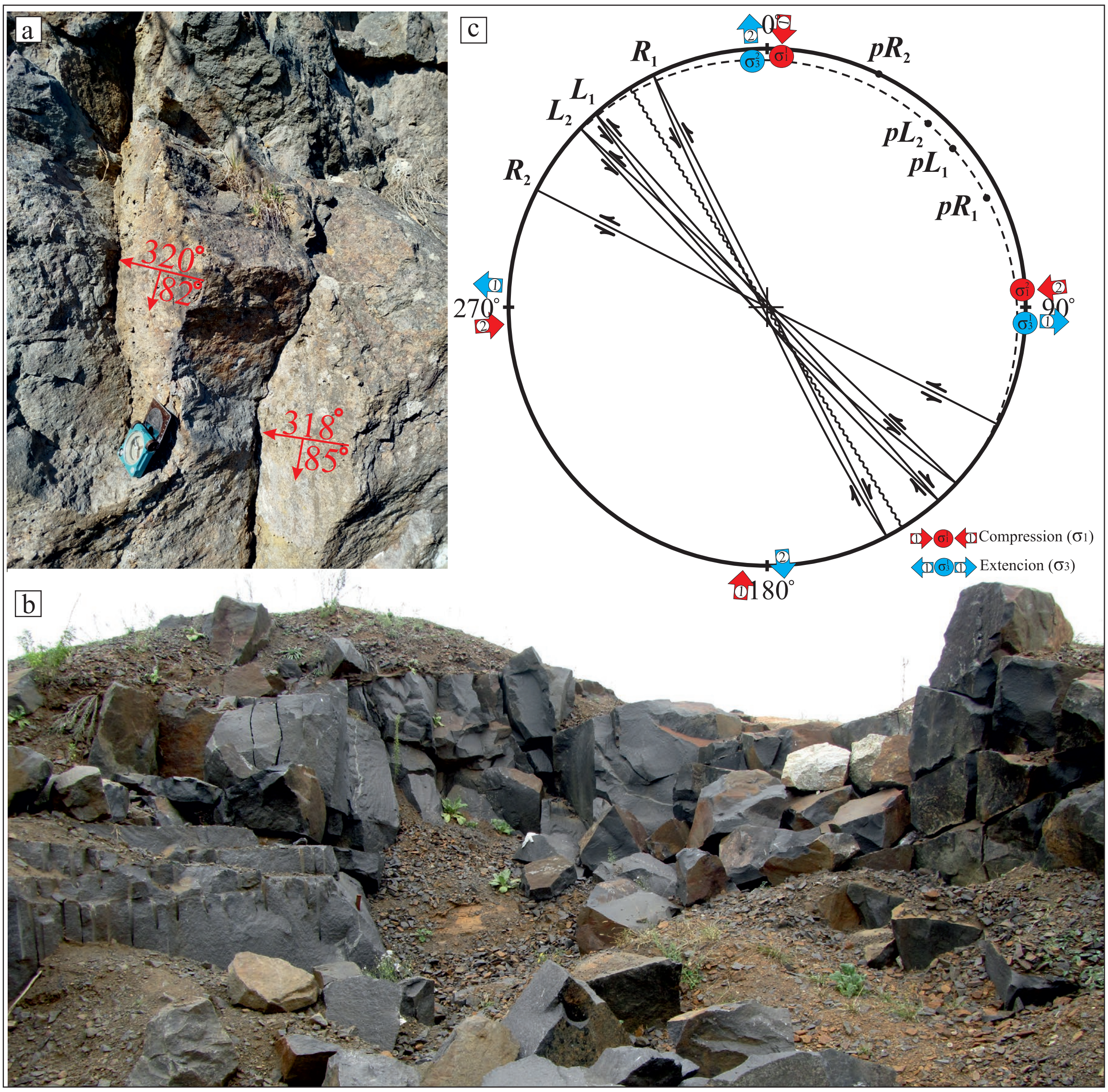

Fig. 8. Results of tectonophysical studies of the Khmilnyk fault zone: **(a)** fracturing of rocks, Vinnytsia; **(b)** gabbro-diabase dyke, Shyroka Hreblya quarry, Khmilnyk; **(c)** results of the inverse kinematic problem for the Khmilnyk fault zone. Photo by S.V. Mychak.

predominantly steep dips, reflecting an overall subvertical geometry consistent with deep-seated reactivation of the Zvizdal–Zalissia fault zone (Mychak et al. 2022).

Although the Zvizdal–Zalissia dyke itself has not been directly dated, its formation is interpreted to be contemporaneous with the emplacement of the Korosten Pluton. This inference is supported by the nearby gabbro-dolerite Rudnya–Bazarska dyke of similar mafic composition, dated at 1793 Ma (Shumlyanskyy et al. 2017), which has been studied in detail regarding its petrostructural characteristics and polybaric crystallization features (Mytrokhyn & Omelchenko 2006; Mitrokhyn et al. 2008). This geochronological marker constrains the extensional phase and associated fault reactivation. Based on 3D gravity models (Figs. 7 and 5b), densities at the depth of 5 km (in the basement) increase southward from 2.60 to 2.78 g cm^{-3} along the Zvizdal–Zalissia zone (Fig. 7a). At 10 and 20 km depths (Fig. 7b, c) within the Korosten region, densities rise from 2.62 to 2.74 and from about 2.78 to 2.86 g cm^{-3}, respectively. At the Moho (Fig. 5b), densities are higher (3.06 g cm^{-3}) in the south and lower (3.00 g cm^{-3}) in the north.

Brusyliv fault zone

The Brusyliv fault zone (Kashperivka–Borshchahivka segment) represents a tectonophysical analogue of the Zvizdal–Zalissia fault zone and is traced subparallel to it at approximately 5 km. The zone deforms biotite and amphibole–biotite plagiogranites that are texturally similar to the rocks of the Zvenyhorodka Complex (2050 Ma; Shcherbak et al. 2008). Density variations with depth within the Brusyliv zone closely resemble those observed in the Zvizdal–Zalissia zone (Fig. 7), indicating comparable deep-crustal architecture. Analysis of fracture-orientation diagrams (Fig. 10c) reveals two principal maxima: A (50°) and E (327°), corresponding to L- and R′-shears, respectively. Additional maxima at B (65°), C (275°), and D (315°) reflect more complex deformation kinematics. Vertical fracture systems define a primary stress field related to the Subottsi–Moshoryne faulting stage (Fig. 10a). Subsequent rotation of the σ_1–σ_3 plane from a subhorizontal to a subvertical position led to the formation of an oblique fracture system (Fig. 10b), indicating progressive reorganization of the stress regime.

Stress-field modeling based on the fracture data yields three possible solutions:

(1) A–E, with σ_1=08°, σ_3=278°, and vertical σ_2;

(2) B–C–D, with σ_1=280°, σ_3=10°, and vertical σ_2;

(3) C–E, with σ_1=301°, σ_3=31°, and vertical σ_2.

These solutions collectively indicate a reverse strike-slip fault regime characterized by sublatitudinal compression (σ_1) and submeridional extension (σ_3), typical of the upper Ros River basin.

At the intersection of the Brusyliv and Nemyriv fault zones, two paleo-stress fields are distinguished: one corresponding to the Nemyriv stage, and another defined by σ_1=301° and σ_3=31°, which coincides with the principal stress field reconstructed for the Novohrad-Volynskyi Massif. The latter stress configuration, best represented by solution 3, is interpreted as the most probable and oldest deformation phase in the Brusyliv fault zone, correlating with deformation of the Novohrad-Volynskyi Massif at ca. 2.05 Ga and predating the stress fields represented by solutions 1 and 2.

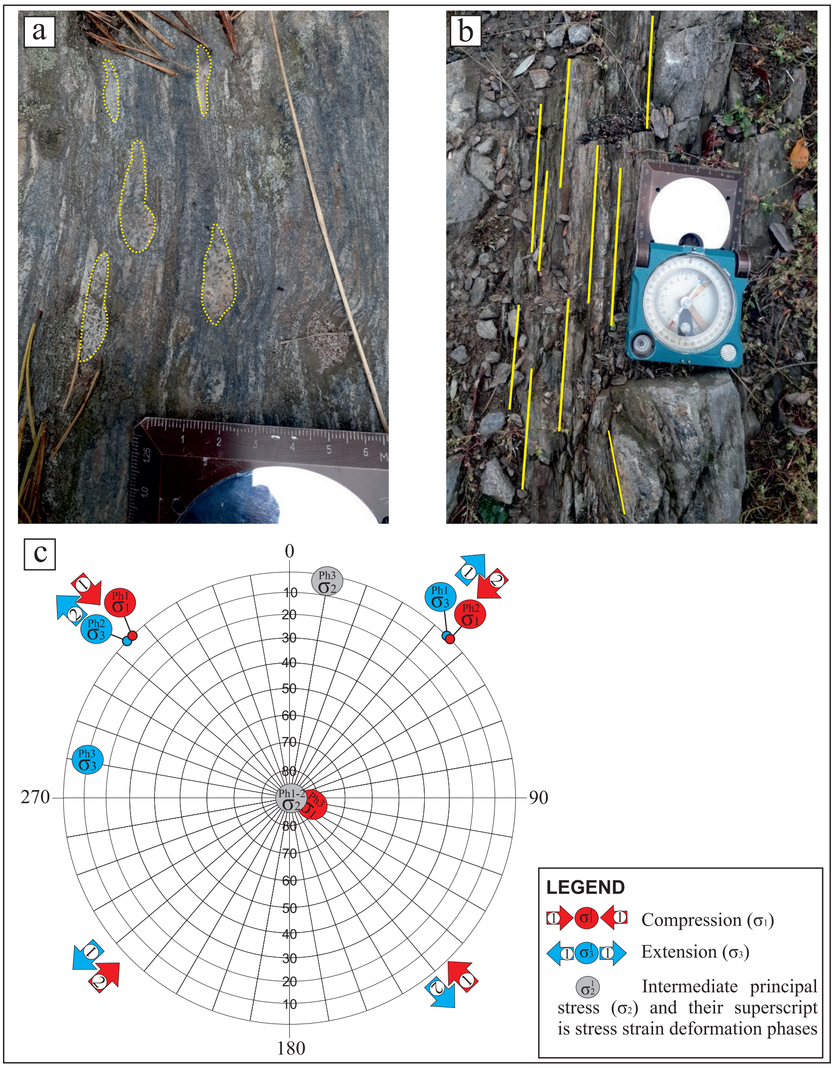

Fig. 9. Results of tectonophysical studies of the of the Zvizdal Zalissia fault zone: **(a)** mineral fragments in metamorphic rock (porphyroclasts) surrounded by a fine-grained matrix, Teteriv River; **(b)** brittle fracturing of rocks and structural/textural elements with a 340° strike azimuth, Teteriv River; **(c)** results of the inverse kinematic problem for the Zvizdal–Zalissia fault zone. Photo by S.V. Mychak.

Bilokorovychi fault zone

This zone represents significant structural boundary dividing the western USh into two parts with contrasting Moho geometry (Fig. 5a). In the west, sinistral strike-slip faults of NE strike (Horyn, Lutsk, Sushchany–Perha, Teteriv, Nemyriv) and E–W faults (Polissia, Volodarsk-Volynskyi, Andrushivka, Khmelnytskyi) bound a system of Moho troughs 50–65 km deep, coinciding with Moho steps that link the troughs. In the east, Moho depths are shallower (40–50 km), with morphology aligned to submeridional Precambrian structures (orthogonal fault system). Maximum density at the Moho (3.20 g cm^{-3}) occurs in the central Bilokorovychi zone (between the Khmilnyk and Sarny–Varvarivka fault zones) and centrally within the block bounded by the NE-trending Ostroh and Teteriv fault zones and the meridional Rivne and Shepetivka fault zones (Fig. 5b). Localized high-density and strong horizontal density gradients occur throughout the crustal column in the Bilokorovychi zone (Figs. 5, 7). In the regional magnetic field (Fig. 11), the Bilokorovychi zone marks a boundary between a western Volyn Domain with positive anomalies and an eastern domain with negative anomalies. A prominent Novograd-Volynskyi regional magnetic anomaly (N–V; ~300 nT) is clear in the southwest. 3D magnetic modelling (Pashkevich et al. 2006; Mychak et al. 2023) indicates a highly magnetized (>50 km thick; ~3 A m^{-1}) lower crust beneath it, surrounded by crustal domains ~40 km thick with reduced lower-crustal magnetization (1–2 A m^{-1}). In eastern

Volyn, a regional magnetic minimum of complex structure combines NW- and NE-trending lows (Fig. 11).

The Bilokorovychi zone attained its role as a structural boundary during the Korosten stage. To the west, where crust is thick and Moho densities are high, dolerite dykes of the Prutivkacomplex and ferro-monzodiorite dykes of the AMCG association occur. To the east lies the Korosten Pluton (also AMCG-type).

During the Subottsi–Moshoryne stage, volcanic rocks of the Bilokorovychi Formation (Topilnia Series) formed in the Bilokorovychi depression at the intersection of the Bilokorovychi and Polissia fault zones (see Fig. 3). Effusives are composed of sub-alkaline basalts and rhyolites (Shcherbakov 2005).

Korosten deformation stage (1.80–1.73 Ga)

This stage is closely associated with the formation of the anorogenic A-type magmatic complexes of the Korosten Pluton. Our tectonophysical data indicate that the emplacement of these voluminous granitic and mafic bodies was fundamentally controlled by a regional extensional stress regime. Alternating phases of sub-latitudinal and sub-meridional extension caused intense fracturing of the crust, reduced lithostatic pressure, and generated permeable channel systems. This extensional geodynamic setting created favourable conditions for the ascent of mantle-derived mafic melts and subsequent crustal melting, which produced the characteristic A-type rapakivi granitoids (Mitrokhyn et al. 2008; Gintov & Mychak 2014).

This stage begins with the formation of two different magmatic associations: the Prutivka and AMCG complexes. The Prutivka Complex comprises layered gabbro, ultramafic bodies and dolerite dykes. The rocks of the AMCG association build the Korosten Pluton and ferro-monzodiorite dykes. Deformation and magmatism during this stage led to widespread replacement and recrystallization of the crust of the western Volyn Block (Bogdanova et al. 2006).

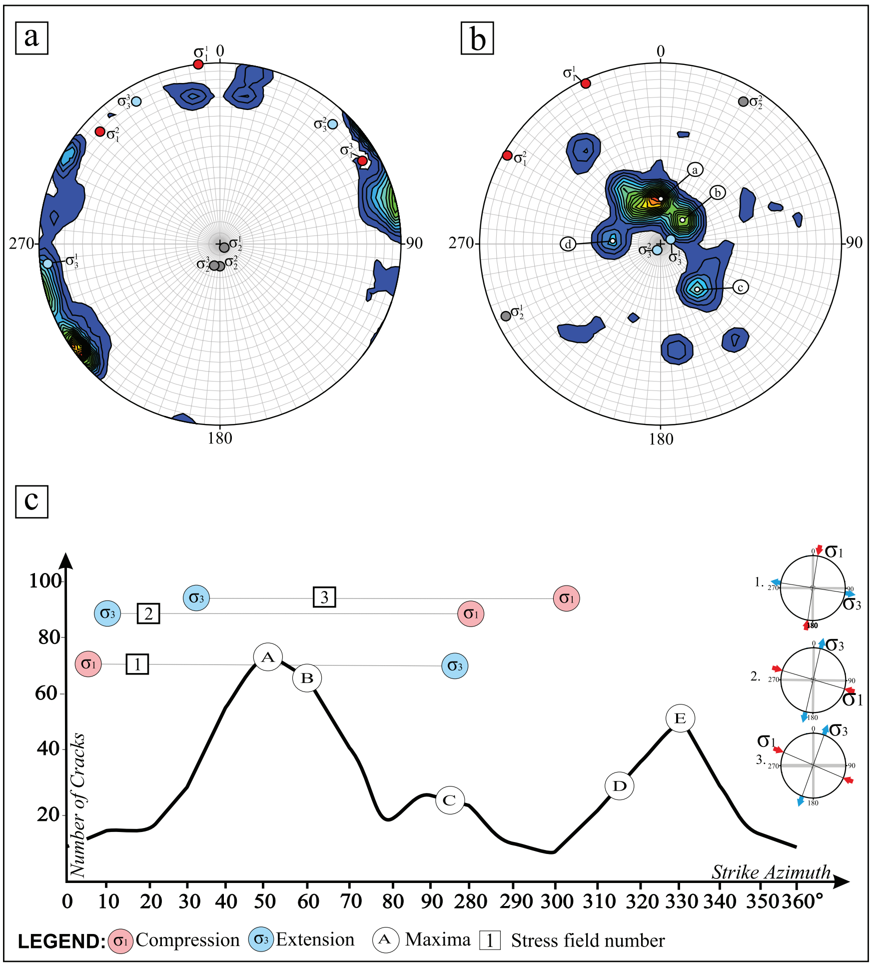

Fig. 10. The results of tectonophysical studies Brusyliv faults zone: **(a)** stereogram of dip directions for vertical fractures, upper course of the Rostavytsia River; **(b)** stereogram of dip directions for inclined fractures, upper course of the Rostavytsia River; **(c)** composite rose diagram (or histogram) of strike azimuths for steeply dipping fractures (>70°) along the Ros River, Brusyliv fault zone (Kashperivka–Borshchahivka segment).

Prutivka dykes and layered bodies are concentrated mainly in the northern and northwestern Volyn Domain (Shcherbak et al. 2008; Shumlyanskyy et al. 2016) (Fig. 3). The formation of the Tomashhorod (1791–1787 Ma) and Sushchany–Perha dyke swarms and as well as the Kamyanka Massif (1788 Ma) and the layered Prutivka sill-like intrusion (1779–1777 Ma) occurred along the meridional Bilokorovychi and diagonal fault zones. The Tomashhorod swarm transects the OMIB, that is segmented at crossings with NE-trending faults and is displaced southwest ward the activation of the Sushchany–Perha fault zone.

Primary melt temperatures for Prutivka rocks exceeded 1490 °C (Shcherbakov 2005), requiring sources at ~250 km depth (Usenko 2025). Their compositions resemble dolerites of Large Igneous Provinces, commonly linked to mantle plume activity (Shumlyanskyy et al. 2016).

The Korosten Pluton and AMCG dykes formed during two magmatic phases, 1810–1770 Ma and 1760–1580 Ma (Shumlyanskyy et al. 2017). Rocks of the Prutivka Complex were emplaced during the first phase (Table 2). A wide range of rock types including anorthosite, gabbro, ferromonzodiorite, and granite is represented in each of the two stages within the Korosten Pluton. Melts originated

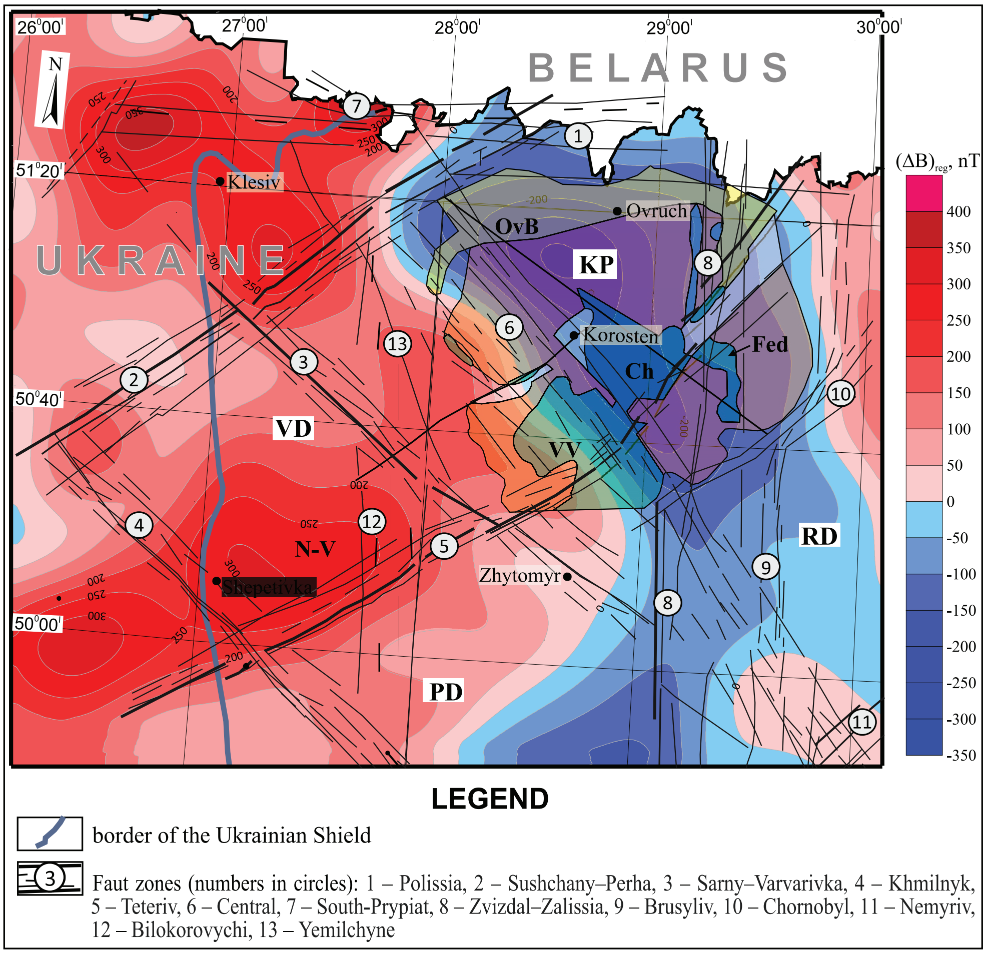

Fig. 11. Map of the regional component of the magnetic field in nT (after Mychak et al. 2022). N-V: Novohrad-Volynskyi regional magnetic anomaly. For other legends see Fig. 1.

both in the crust and at the crust-mantle boundary. Ferromonzonite/monzodiorite dykes occur within the pluton and extend far to the west. Inside the massif, these dykes are concentrated along the Sarny–Varvarivka and Central fault zones.

The oldest Korosten Pluton rocks (granites; 1817 Ma) are localized along the Ovruch Basin. At its intersections with the Central and Bilokorovychi fault zones formed the Yastrebetsky (1772 Ma) and with the Zvizdal–Zalissia zone the Davydky (1789 Ma) Massifs of alkaline rocks (Fig. 3). At the Zvizdal–Zalissia–Teteriv intersection the Rudnya-Bazarska and Bilokorovychi ferro-monzodiorite dykes formed at 1793 Ma. Early anorthosites of the Fedorivka Massif (1784–1781 Ma) occur along the Zvizdal–Zalissia fault zone. Separate bodies of early anorthosites (for example the Pugachivka dyke, 1800 Ma) are located within the Central fault zone (Shumlyanskyy et al. 2017).

Most of the magmatic rocks of the Korosten Pluton – including wehrlites, gabbros, and anorthosites of the Volodarsk-Volynskyi and Chopovychi massifs, as well as most of the granites, including rapakivi granites – formed during the second deformation phase (Shcherbakov 2005). Monzodiorite bodies crystallized within the Korosten Pluton and the Buky Massif, where they are assigned to the Strybizh Complex 1758–1761 Ma (Table 2; Shcherbakov 2005; Shumlyanskyy 2012). Their emplacement was structurally controlled by the Teteriv Fault Zone and its intersection with the Central Fault Zone within the pluton, and by the Sarny–Varvarivka Fault Zone within the Buky Massif. Granitic magmatism, including the emplacement of rare-metal granites, continued until approximately 1743 Ma (Shumlyanskyy et al. 2017).

Tectonophysical analysis of fractures in Korosten Pluton gabbro, gabbro–anorthosite, and rapakivi granite reveals well-defined orientation maxima that correspond to systematic shear-fracture sets (Fig. 12). Subvertical fractures form characteristic systems of Riedel shears (R and R′), together with L- and L′-shears and, more rarely, P- and P′-shears. Histograms of fracture strike azimuths obtained from both gabbro–anorthosites and rapakivi granites show consistent maxima, indicating that these lithologies record a common stress field during deformation and cooling of the pluton.

The main orientation maxima are as follows: L- and L′-shears at 287° and 18° (B–B′, E–E′); R- and R′-shears at 298° and 358° (C–C′, D–D′); and P- and P′-shears at 273° and 31° (A–A′, F–F′). Interpretation of these fracture systems

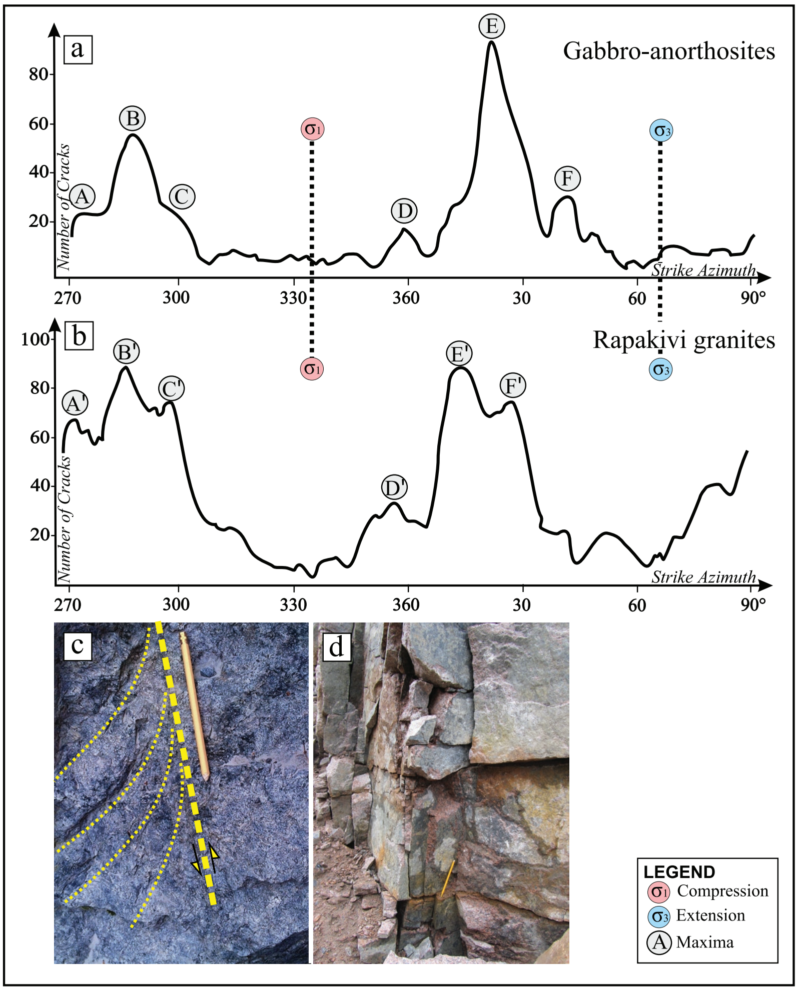

Fig. 12. Results of tectonophysical studies of the Korosten Pluton: **(a–b)** frequency distribution of fracture strike azimuths in gabbro-anorthosites and rapakivi granites; **(c)** relationship between fractures and the crystal fabric of rapakivi granites (Open-pit № 6, Malyn); thin yellow dashed lines indicate the reorientation of plagioclase crystals forming upturning structures due to sinistral strike-slip deformation along the fracture; **(d)** vertical fracturing in Rapakivi granites. Photo by S.V. Mychak.

indicates that the Korosten Pluton formed and cooled under a regional extensional stress regime, with the principal stress axes oriented at σ_1=333° and σ_3=63°. The development of these fracture systems occurred during pluton cooling at depths of approximately 2–5 km under brittle to quasi-brittle conditions (Gintov & Mychak 2014).

Magmatic activity in the Volyn Domain concluded with the eruption of rhyolites in the Ovruch Basin at ca. 1761 Ma along the Polissia zone. In addition to rhyolites, the Zbranky Suite of the Ovruch Series contains metabasalts and metatrachyandesites (Shcherbak et al. 2008; Shumlyanskyy et al. 2017).

Fracture measurements within the Zbranky Suite define two distinct stress fields. An early field (σ_1=158/08, σ_3=248/03, σ_2=30/86°) closely matches the stress state inferred for the Korosten Pluton's gabbro–anorthosites and rapakivi granites, with principal axis orientations differing by only ~5°. A late field (σ_1=270/05, σ_3=360/00, σ_2=90/85°) possibly reflects a strike-slip fault regime with meridional extension, potentially associated with the formation of either the Ovruch or the Prypiat basins (Gintov & Mychak 2014).

Conclusions

The tectono-magmatic evolution of the western USh during 2.05–1.73 Ga progressed through well-defined stages accompanied by large-scale deformation, changes in the crustal stress–strain state, and intense magmatism against the backdrop of collision among Fennoscandia, Sarmatia, and Volgo-Uralia.

Formation of the Sushchany–Perha, Nemyriv, Khmilnyk, Zvizdal–Zalissia, Brusyliv, and other fault zones is closely linked to phases of magmatic activity and shifts in the regional tectonic stress field. These zones underwent multiple reactivations, showing changes in deformation mode and direction and periods of enhanced permeability for melts and fluids.

The Nemyriv and Sushchany–Perha fault zones made an important contribution to the Paleoproterozoic regional evolution. During the early deformation stages (2.0–1.9 Ga), the Nemyriv Fault Zone acted as a major structural lineament and functioned as a large sinistral strike-slip and thrust boundary that facilitated the collisional amalgamation and tectonic integration of the Podolian and Ros' domains. In contrast, during the subsequent stages (1.80–1.73 Ga), the Sushchany–Perha Fault Zone played a dominant role as a deep, highly permeable sinistral strike-slip and extensional conduit system operating within a regional extensional stress field. This fault zone exerted structural control over the localization of late Paleoproterozoic anorogenic magmatism, including rare-metal mineralization, and contributed significantly to the development of the present-day physical properties and segmented crustal architecture of the western Ukrainian Shield.

Crustal density heterogeneity is governed by two principal fault systems: a NE-trending set (e.g., Teteriv and Sushchany–Perha) reflecting coupling at the Sarmatia–Fennoscandia junction, and an E–W (sub-latitudinal) set (e.g., Polissia and Volyn) forming a throughgoing belt related to the Prypiat Trough (the Prypiat–Brest fault zone).

The meridional Bilokorovychi fault zone is established as a structural boundary dividing the western USh into two parts: western and eastern. Both differ significantly in different density and magnetic properties, as well as in the thickness of the crust. The western part is characterized by thicker crust (up to 60 km), positive regional magnetic anomalies achieving values up to +350 nT and higher densities on Moho (up to 3.12 g cm^{-3}). On the other hand, the eastern part is represented by thinner crust (only 40–50 km), mostly negative magnetic anomalies, which reach values of −350 nT within the Korosten Pluton area, and lower density values at the Moho (2.98–3.06 g/cm³). This zone warrants dedicated geological–geophysical study to refine the tectonic history and present structure of the western part of the USh.

Magmatic melts formed between 2.05 and 1.73 Ga were of both mantle and crustal origin. This is confirmed by both geochemical and isotopic characteristics of intrusive and volcanic rocks. The coexistence of mafic-ultramafic and granitoid complexes indicates a close interaction of mantle and crustal sources of melts in the zone of tectonic activity. Geological–geophysical data show that large linear dyke swarms are localized at contacts between crustal blocks of contrasting composition.

Emplacement of the Korosten Pluton of gabbro–anorthosite and rapakivi granite represents the culminating event in the tectono-magmatic development of the western part of USh. Its multiphase formation (1.81–1.73 Ga) was accompanied by extensive dyke swarms across much of the Volyn Domain.

After the Subottsi–Moshoryne and Korosten stages of faulting, no subsequent strong deformation has been recognized within the USh.

Acknowledgements: This research was supported by the Slovak Research and Development Agency under the contracts Nos. APVV-SK-UA-25-0003, APVV-24-0445, and the VEGA Slovak Grant Agency under project Nos. 2/0002/23, 1/0107/23. Authors are grateful to Prof. Dušan Plašienka and Dr. Milan Kohút for valuable advice while writing this paper. The work was also carried out within the framework of bilateral scientific cooperations between the National Academy of Sciences of Ukraine and the Slovak Academy of Sciences (SAS–NASU 2025-01).

References

Allmendinger R.W., Cardozo N. & Fisher D. 2012: *Structural geology algorithms: vectors and tensors*. Cambridge University Press, 1–304.

Bogdanova S.V., Pashkevich I.K., Gorbatschev R. & Orlyuk M.I. 1996: Riphean rifting and mojor Palaeoproterozoic crustal boundaries in the basement of the East European Craton: geology and geophysics. *Tectonophysics* 268, 1–21, https://doi.org/10.1016/S0040-1951(96)00232-6

Bogdanova S., Gorbatschev R., Grad M., Guterch A., Janik T., Kozlovskaya E., Motuza G., Skridlaite G., Starostenko V. & Taran L. 2006: EUROBRIDGE: new insight into the geodynamic evolution of the East European Craton. In: Gee D.G., Stephenson R.A. (Eds.): European Lithosphere Dynamics. *Geological Society, London, Memoirs* 32, 599–628. https://doi.org/10.1144/gsl.mem.2006.032.01.36

Bogdanova S.V., Gintov O.B., Kurlovich D., Lubnina N.V., Nilsson M., Orlyuk M.I., Pashkevich I.K., Shumlyanskyy L.V. & Starostenko V.I. 2013: Late palaeoproterozoic mafic dyking in the Ukrainian Shield (Volgo-Sarmatia) caused by rotations during the assembly of supercontinent Columbia. *Lithos* 174, 196–216, doi.org/10.1016/j.lithos.2012.11.002

Cammani G., Chalds C., Delogkos E., Roche V., Manzocci T. & Walsh J. 2023: The role of antithetic faults in transferring displacement across contractional relay zones on normal faults. *Journal of Structural Geology* 168, 104827. https://doi.org/10.1016/j.jsg.2023.104827

Delvaux D., Rikkert Moeys R., Stapel G., Petit C., Levi K., Miroshnichenko A., Ruzhich V. & San'kov V. 1997: Paleostress reconstructions and geodynamics of the Baikal region, Central Asia, Part 2. Cenozoic rifting. *Tectonophysics* 282, 1–38, https://doi.org/10.1016/S0040-1951(97)00210-2

Dooley T.P. & Schreurs G. 2012: Analogue modelling of intra-plate strike-slip tectonics: A review and new experimental results. *Tectonophysics* 574, 1–71. https://doi.org/10.1016/j.tecto.2012.05.030

Entin V.A. 2005: Geophysical basis of the Tectonic Map of Ukraine at a scale of 1:1000 000 (in Russian). *Geofizicheskiy Zhurnal* 27, 1, 74—88.

Entin V.A., Shimkiv L.M., Nechayeva T.S., Dzyuba B.M., Gintov O.B., Pashkevich I.K. & Krasovskiy S.S. 2002: *Preparation of the geophysical basis of the tectonic map of Ukraine of scale 1:100 000*. Geoinform of Ukraine, Kyiv, 1–55 (in Ukrainian).

Gintov O.B. 2005: Field tectonophysics and its application in the study of deformations of the earth's crust in Ukraine (in Russian). *Feniks*, Kiev, 572.

Gintov O.B. & Mychak S.V. 2014: Kinematics of formation of the Ukrainian Shield during the period 1,80–1,73 Ga ago according to the results of studies of rock fracturing of the Korosten and Korsun-Novomirgorod plutons (in Russian). *Geofizicheskiy Zhurnal* 36, 24–36. https://doi.org/10.24028/gzh.0203-3100.v36i4.2014.116006

Gintov O.B. & Pashkevich I.K. 2010: Tectonophysical analysis and geodynamic interpretation of the three-dimensional geophysical model of the Ukrainian shield. *Geofizicheskiy Zhurnal* 32, 3–27 (in Russian).

Gintov O.B., Orlyuk M.I., Entin V.A., Pashkevich I.K., Mychak S.V., Bakarzhieva M.I., Shimkiv L.M. & Marchenko A.V. 2018: The structure of the Western and Central parts of the Ukrainian schield. Controversial issues. *Geofizicheskiy Zhurnal* 40, 3–29 (in Ukrainian). https://doi.org/10.24028/gzh.0203-3100.v40i6.2018.151000

Heidbach O., Tingay M., Barth A., Reinecker J., Kurfeß D. & Mülle B. 2010: Global crustal stress pattern based on the World Stress Map database release 2008. *Tectonophysics* 482, 3–15. https://doi.org/10.1016/j.tecto.2009.07.023

Kostenko M.M. 2019: Metallogenic features and prospects for ore bearing of basic dike complexes of the Volyn megablock of the Ukrainian Shield (in Ukrainian). *Collection of scientific papers of the UkrSDGR* 3–4, 9–23.

Kovalenko-Zavoysky V.M. & Ivashchenko I.M. 2006: Mathematical support for the interpretation of the field $\Delta \boldsymbol{B}_a$ of the regional magnetic anomalies. *Geofizicheskiy Zhurnal* 28, 18–29.

Krylov I.A. (Ed.) 1988: *Map of discontinuities and main zones of lineaments in the southwest of the USSR (using satellite imagery).* Scale 1:1000 000. Edition of the Main Directorate of Geodesy and Cartography, Moscow, 1–4 (in Russian).

Kryvdik S.G., Tsymbal S.N. & Gejko Y.V. 2003: Proterozoic alkaline ultramafic magmatism of the North-Western region of the Ukrainian shield as an indicator of formation of kimberlites. *Mineralogical journal (Ukraine)* 25, 57–69 (in Russian).

Lund B. & Zoback M.L. 1999: Orientation and magnitude of *in situ* stress to 6.5 km depth in the Baltic Shield. *International Journal of Rock Mechanics and Mining Sciences* 36, 169–190. https://doi.org/10.1016/S0148-9062(98)00183-1

Makarenko I.B., Starostenko V.I., Kuprienko P.Ya., Savchenko O.S. & Legostaeva O.V. 2021: *Heterogeneity of the Earth's crust of Ukraine and adjacent regions according to the results of 3D gravity modeling (in Ukrainian)*. Naukova Dumka, Kyiv, 1–204.

Makarenko I., Legostaeva O., Savchenko O., Starostenko V. & Zadyraka O. 2023: Modern technology of 3D gravity modeling. In: *XVII International Scientific Conference "Monitoring of Geological Processes and Ecological Condition of the Environment"*. November 7–10, 2023, Kyiv, Ukraine. https://doi.org/10.3997/2214-4609.2023520018

Mychak S.V. 2014: Rock deformation of the Uman, Novohrad-Volynskyi and Novoukrainskyi massifs in the period of 2.02–2.05 Ga by the results. *Geodynamika* 2, 150–162 (in Ukrainian). https://doi.org/10.23939/jgd2014.02.150

Mychak S. & Farfuliak L. 2021: Inner structure and kinematics of the Sushchany-Perga fault zone of the Ukrainian Shield according to the tectonophysical study. *Geofizicheskiy Zhurnal* 43, 142–159. https://doi.org/10.24028/gzh.0203-3100.v43i1.2021.225496

Mychak S., Kurylo S., Belskyi V. & Murovskaya A. 2016: Stress-strain state of Rosynsk block of the shield for upstream of the Ros'river (Fursy – Borschahivka). *Geodynamics* 21, 123–133 (in Ukrainian). https://doi.org/10.23939/jgd2016.02.123

Mychak S., Bakarzhyeva M., Farfuliak L. & Marchenko A. 2022: The inner structure and kinematics of the Zvizdal-Zalisk and Brusyliv fault zones of the Ukrainian shield by the results of tectonophysical, magnetometrical data. *Geofizicheskiy Zhurnal* 44, 83–110 (in Ukrainian). https://doi.org/10.24028/gzh.v44i1.253712

Mychak S.V., Bakarzhieva M.I., Usenko O.V. & Marchenko A.V. 2023: The Volyn Domain of the Ukrainian Shield (East European Craton): multiple stress changes during the Palaeoproterozoic tectonic evolution. In: *17th International Conference Monitoring of Geological Processes and Ecological Condition of the Environment*. Nov. 2023, Ukraine Kyiv, 1–5, https://doi.org/10.3997/2214-4609.2023520099

Mytrokhyn O. & Omelchenko A. 2006: Petrography of gabbro-dolerites of Zvizdal-Zalesye dyke. *Visnyk of Taras Shevchenko National University of Kyiv, Geology* 36, 30–32. https://geology.bulletin.knu.ua/en/article/view/3389/2889

Mytrokhyn O.V., Bohdanova S.V. & Shumlyanskyy L.V. 2008: Polybaric crystallization of anorthosites from the Korosten Pluton (Ukrainian Shield). *Mineralogical Journal* 30, 36–52 (in Russian).

Pashkevich I.K., Orlyuk M.I., Eliseeva S.V., Bakarzhieva M.I., Lebed T.V. & Romenets A.A. 2006: 3D magnetic model of the Earth's crust of the Ukrainian Shield and its petrological and tectonic interpretation (in Russian). *Geofizicheskiy Zhurnal* 28, 7–18.

Scheme of gravity field of Ukraine, 1:1 000 000 2002: *Northern State Regional Geological Enterprise "Northern Geology" of Natural Resources of Ukraine* (in Ukrainian).

Shcherbak N.P., Artemenko G.V., Lesnaya I.M., Ponomarenko A.N. & Shumlyanskyy L.V. 2008: *Geochronology of the Early Precambrian of the Ukrainian Shield. Proterozoic*. Naukova Dumka, Kiev, 1–240 (in Russian).

Shcherbakov I.B. 2005: *Petrology of the Ukrainian Shield*. ZUKTS, Lviv, 1–366 (in Russian).

Shumlyanskyy L.V. 2012: *Petrology and geochronology of rock complexes of the Northwestern region of the Ukrainian Shield and its western slope*. Doc. Geol. Sci. Dissertation, Kyiv, 1–510 (in Ukrainian).

Shumlyanskyy L.V. 2014: Geochemistry of the Osnitsk-Mikashevichy volcanoplutonic complex of the Ukrainian shield. *Geochemistry International* 52, 912–924. https://doi.org/10.1134/S0016702914110081

Shumlyanskyy L., Ernst R.E., Söderlund U., Billström K., Mitrokhin O. & Tsymbal S. 2016: New U–Pb ages for mafic dykes in the Northwestern region of the Ukrainian shield: coeval tholeiitic and jotunitic magmatism. In: Issue 1: New advances in using Large Igneous Provinces (LIPs) to reconstruct ancient supercontinents. *GFF* 138, 79–85. https://doi.org/10.1080/11035897.2015.1116602

Shumlyanskyy L., Hawkesworth C., Billstrom K., Bogdanova S., Mytrokhyn O., Romer R., Dhuime B., Claesson S., Ernst R., Whitehouse M. & Bilan O. 2017: The origin of the Palaeoproterozoic AMCG complexes in the Ukrainian shield: New U-Pb ages and Hf isotopes in zircon. *Precambrian Research* 292, 216–239. https://doi.org/10.1016/j.precamres.2017.02.009

Shumlyanskyy L.V., Stepaniuk L.M., Claesson S., Rudenko K.V. & Becker A.Yu. 2018: U–Pb on zircon and monazite geochronology of granites of the Zhytomyr and Sheremetiv complexes, the north-western region of the Ukrainian shield. *Mineralogical Journal* 40, 63–85. https://doi.org/10.15407/mineraljournal.40.02.063

Stepanyuk L.M. 2024: *Monazitometry of the Ukrainian Shield (Volyn and Dniester-Bug megablocks)*. Akademperiodyka, Kyiv, 1–232 (in Ukrainian). https://doi.org/10.15407/akademperiodyka.514.232

Stepanyuk L.M., Ponomarenko O.M., Petrichenko K.V, Kurilo S.I., Dovbush T.I., Sergeev S.A. & Rodionov N.B. 2015: Uranium–lead isotopic geochronology of Berdychiv-type granitoids of the Bug area (The Ukrainian Shield). *Mineralogical Journal* 37, 51–66. https://doi.org/10.15407/mineraljournal.37.03.051

Stepanyuk L.M., Vysotsky O.B., Dovbush T.I., Bilan O.B. & Kovalenko N.O. 2020: Geochronology of magmatic rocks of Osnitsk block (Ukrainian shield) on zircon and titanite *Mineralogical Journal* 42, 66–75. https://doi.org/10.15407/mineraljournal.42.01.066

Usenko O. 2024: Thermodynamic conditions of granitization and metamorphism of rocks in the northwestern part of the Ukrainian shield (in Ukrainian). *Geofizicheskiy Zhurnal* 46, 34–52. https://doi.org/10.24028/gj.v46i2.294984

Usenko O. 2025: Reconstruction of the deep process based on the analysis of the magmatic rocks composition (on the example of the Osnytsk and Buky complexes of the Volyn megablock of the Ukrainian Shield) (in Ukrainian). *Geofizicheskiy Zhurnal* 47, 50–82. https://doi.org/10.24028/gj.v47i1.309811

Vysotsky O.B., Stepanyuk L.M., Dovbush T.I. & Kovalenko N.O. 2020: U–Pb geochronology by zircon of fine-grained granite of the Osnitsky complex. (Volinsky megablok US). *Geochemistry and Ore Formation* 41, 83–86. https://doi.org/10.15407/gof.2020.41.083

Zang A. & Stephansson O. 2010: *Stress field of the Earth's crust*. Springer, 1–322. https://doi.org/10.1007/978-1-4020-8444-7

Zoback M.L. & Zoback M.D. 1989: Chapter 24: Tectonic stress field of the continental United States. *Geological Society of America Memoirs* 172, 523–540.